เอสเทอริฟิเคชันกรดไขมันอิสระด้วยตัวเร่งปฏิกิริยาวิวิธพันธุ์ชนิดกรดในเครื่องปฏิกรณ์ต่อเนื่องแบบแพ็กเบด

นายสมยศ เกศโพคะศิริ

วิทยานิพนธ์นี้เป็นส่วนหนึ่งของการศึกษาตามหลักสูตรปริญญาวิทยาศาสตรมหาบัณฑิต
สาขาวิชาปิโตรเคมีและวิทยาศาสตร์พอลิเมอร์
คณะวิทยาศาสตร์ จุฬาลงกรณ์มหาวิทยาลัย
ปีการศึกษา 2554

FREE FATTY ACID ESTERIFICATION USING ACIDIC HETEROGENEOUS CATALYST IN CONTINUOUS PACKED BED REACTOR

Mr. Somyod Kedpokasiri

A Thesis Submitted in Partial Fulfillment of the Requirements
for the Degree of Master of Science Program in Petrochemistry and Polymer Science
Faculty of Science
Chulalongkorn University
Academic Year 2011

Thesis Title	FREE FATTY ACID ESTERIFICATION USING ACIDIC HETEROGENEOUS CATALYST IN CONTINUOUS PACKED BED REACTOR
By	Mr. Somyod Kedpokasiri
Field of Study	Petrochemistry and Polymer Science
Thesis Advisor	Duangamol Tungasmita, Ph.D.

Accepted by the Faculty of Science, Chulalongkorn University in Partial Fulfillment of the Requirements for the Master's Degree

……..Dean of the Faculty of Science

(Professor Supot Hannongbua, Dr. rer. nat.)

THESIS COMMITTEE

……..Chairman

(Professor Pattarapan Prasassarakich , Ph.D.)

……..Thesis Advisor

(Duangamol Tungasmita, Ph.D.)

……..Examiner

(Associate Professor Wimonrat Trakarnpruk, Ph.D.)

……..External Examiner

(Anurak Winitsorn, Ph.D.)

สมยศ เกศโพคะศิริ : เอสเทอริฟิเคชันกรดไขมันอิสระด้วยตัวเร่งปฏิกิริยาวิวิธพันธุ์ชนิดกรดในเครื่องปฏิกรณ์ต่อเนื่องแบบแพ็กเบด (FREE FATTY ACID ESTERIFICATION USING ACIDIC HETEROGENEOUS CATALYST IN CONTINUOUS PACKED BED REACTOR) อ. ที่ปรึกษาวิทยานิพนธ์หลัก: ดร. ดวงกมล ตุงคสมิต, 87 หน้า.

ได้เตรียมเบนโทไนท์ด้วยวิธีการแลกเปลี่ยนไอออนกับกรดซัลฟูริกความเข้มข้น 0.5 โมลาร์ นำเบนโทไนท์มาตรวจสอบลักษณะเฉพาะด้วยเทคนิคเอ็กซ์เรย์ฟลูออเรสเซนส์ เทคนิคเอ็กซ์เรย์ดิฟแฟรกชัน อินฟราเรดสเปกโทรสโคปี กล้องจุลทรรศน์แบบส่องกราด การดูดซับแก๊สไนโตรเจน และวิเคราะห์การสลายตัวทางความร้อน ทำปฏิกิริยาเอสเทอริฟิเคชันของกรดโอเลอิก 15 เปอร์เซนต์โดยน้ำหนักในน้ำมันปาล์มที่ผ่านการกลั่นกับแอลกอฮอล์ โดยใช้ตัวเร่งปฏิกิริยาเบนโทไนท์ในเครื่องปฏิกรณ์ต่อเนื่องแบบแพ็กเบด ได้ศึกษาผลของภาวะปฏิกิริยาต่างๆ ได้แก่ อัตราส่วนโดยโมลของกรดโอเลอิกต่อแอลกอฮอล์ ปริมาณกรดไขมันอิสระเริ่มต้น ความสูงของตัวเร่งปฏิกิริยาและอุณหภูมิในการเกิดปฏิกิริยา ภาวะที่เหมาะสมที่สุดคืออัตราส่วนโมลของกรดโอเลอิกต่อแอลกอฮอล์เท่ากับ 54 ความสูงของตัวเร่งปฏิกิริยา 25 เซนติเมตร(น้ำหนัก 13.5 กรัม) ที่อุณหภูมิ 60 องศาเซลเซียส สำหรับ 1 คอลัมน์ ได้อัตราการเปลี่ยนแปลงกรดไขมันอิสระสูงสุดเป็น 92.6 และ 94.9 เปอร์เซ็นต์ สำหรับเมทานอลและเอทานอลตามลำดับ นอกจากนี้อัตราการเปลี่ยนแปลงกรดไขมันอิสระสูงสุดเป็น 78.3 และ 86.6 เปอร์เซ็นต์ สำหรับปฏิกิริยาเอสเทอริฟิเคชันของน้ำมันสบู่ดำกับเมทานอลและเอทานอลตามลำดับ เมื่อนำเอทานอลมาใช้ พบว่าเอทานอลให้อัตราการเปลี่ยนแปลงกรดไขมันอิสระสูงกว่าเมทานอล เนื่องจากการละลายเพิ่มขึ้นระหว่างน้ำมันและแอลกอฮอล์ ความว่องไวในการเร่งปฏิกิริยาของตัวเร่งปฏิกิริยาที่ผ่านการใช้งานแล้วลดลง เนื่องจากมีการหลุดของกรดและการสลายของมอนต์มอริลโลไนต์ในโครงสร้าง

สาขาวิชา ปิโตรเคมีและวิทยาศาสตร์พอลิเมอร์ ลายมือชื่อนิสิต .....

ปีการศึกษา 2554 ลายมือชื่อ อ.ที่ปรึกษาวิทยนิพนธ์หลัก .....

5272574323: MAJOR PETROCHEMISTRY AND POLYMER SCIENCE
KEYWORDS: BENTONITE CLAY / ESTERIFICATION / PACKED-BED REACTOR / BIODIESEL

SOMYOD KEDPOKASIRI: FREE FATTY ACID ESTERIFICATION USING ACIDIC HETEROGENEOUS CATALYST IN CONTINUOUS PACKED BED REACTOR. ADVISOR: DUANGAMOL TUNGASMITA, Ph.D., 87 pp.

Bentonite clay was treated with 0.5 M H_2SO_4 by ion-exchange method. The treated bentonite was characterized by x-ray fluorescence spectroscopy (XRF), x-ray powder diffraction (XRD), infrared spectroscopy (IR), scanning electron microscopy (SEM), N_2 adsorption-desorption and thermogravimetric analysis (TGA). Esterification of 15 wt% oleic acid in refined palm oil with alcohol was treated over bentonite as catalyst in a continuous packed bed reactor. The various reaction conditions such as mole ratio of oleic acid to alcohol, amount of initial free fatty acid, catalyst height and reaction temperature were studied. The optimum condition of oleic acid was performed under mole ratio of alcohol to oleic acid as 54, catalytic height 25 cm (13.5 g) at 60°C in one column experiment. The highest FFA conversion was obtained at 92.6% and 94.9% for methanol and ethanol, respectively. Meanwhile, the highest FFA conversions were 78.3% and 86.6% for *Jatropha curcas* oil esterification with methanol and ethanol, respectively. When ethanol was used, FFA conversion was higher than methanol due to increasing solubility between oil and alcohol. The catalytic activity of reused catalyst was decreased due to acid leaching and decomposition of montmorillonite structure.

Field of Study: Petrochemistry and Polymer Science Student's Signature .....

Academic Year: 2011 Advisor's Signature .....

ACKNOWLEDGEMENTS

The success of this thesis can be attributed to the extensive support, valuable suggestion and assistance from my thesis advisor, Dr. Duangamol Tungasmita. I deeply thank her for kindness throughout this study.

I would like to sincerely thank the chairman and the thesis committees for all of their comment and useful suggestion about this research.

I would like to gratefully thank the financial support from PTT Public Company Limited. I am grateful to Program of Petrochemistry and Polymer Science, Faculty of Science, Chulalongkorn University for the valuable knowledge and experience. Moreover, I deeply appreciate National Center of Excellence for Petroleum, Petrochemicals, and Advanced Materials (NCE-PPAM) for partial lab expense supporting.

Many thanks go in particular to the members of Materials Chemistry and Catalysis Research Unit and my friends for their sincere help and kindness. Finally, I deeply wish to thank my family for their entirely care and understanding during my graduate study.

CONTENTS

CHAPTER **Page**

CHAPTER **Page**

LIST OF TABLES

Table **Page**

LIST OF FIGURES

Figure **Page**

Figure **Page**

LIST OF SCHEMES

Scheme **Page**

LIST OF ABBREVIATIONS

BET	Brunauer-Emmett-Teller
BJH	Barret, Joyner, and Halenda
^{o}C	Degree Celsius
g	Gram (s)
hr	Hour (s)
cm	Centimeter
μm	Micrometer (s)
ml	Milliliter (s)
min	Minute (s)
M	Molarity
nm	Nanometer (s)
%	Percentage
SEM	Scanning Electron Microscopy
XRD	X-ray Diffraction
XRF	X-ray Fluorescence Spectroscopy
TGA	Thermogravimetric Analysis
IR spectroscopy	Infrared spectroscopy
LHSV	Liquid Hourly Space Velocity

CHAPTER I

INTRODUCTION

1.1 Background

Energy consumption of the world is projection to increase by 44 percent per year, from 472 quadrillion Btu in 2006 to 678 quadrillion Btu in 2030 (figure 1.1). The world energy needs are supplied through petrochemical sources, natural gases and coal. Diesel fuel marks an essential function in the industrial economy, transportation, agricultural goods, etc. The diesel fuel demand has been increasing as well as the economic growth. However continuing and increasing use of petroleum will intensify air pollution, since NO_X, CO_2 (greenhouse gas) and particulates of exhausted from diesel engine. Consequently, the search for clean alternative energy which is renewable and environment-friendly has been carried out. Biodiesel is one an alternative energy due to a renewable energy, low emission particles, biodegradable and non-toxic. Figure 1.2 shows the world biodiesel capacity between 1991 and 2010.

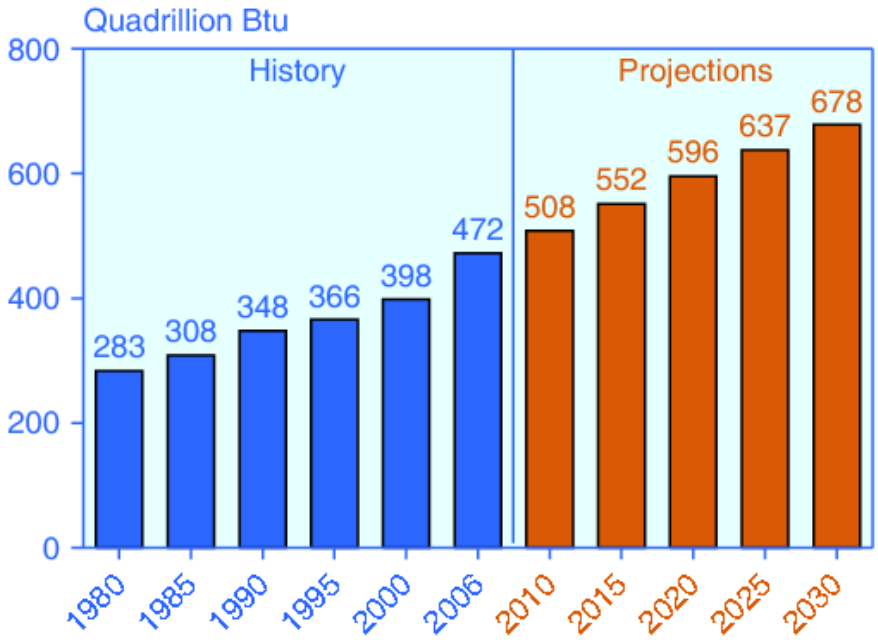

Figure 1.1 World marketed energy consumption, 1980-2030 [1].

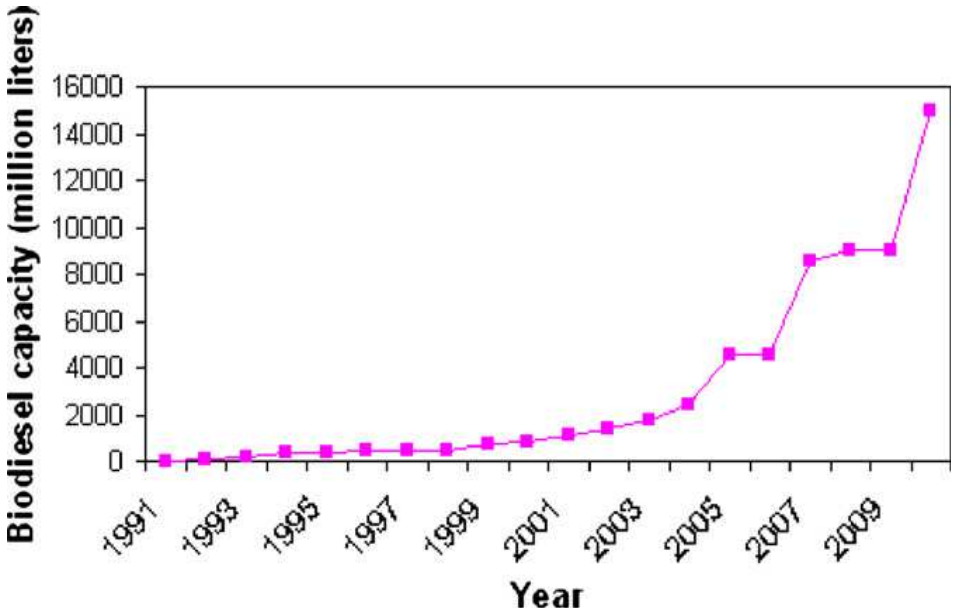

Figure 1.2 World biodiesel capacity, 1991-2010 [2].

Mostly, biodiesel production was produced from oil feedstock like vegetable oil, animal fats or recycle cooking oil. There is usually made through a chemical process called transesterification and esterification whereby triglycerides and free fatty acid react with low molecular weight alcohols, typically methanol or ethanol in the presence catalyst to produce a complex mixture of fatty acid alkyl esters (biodiesel). Catalysts used for the esterification of free fatty acid are classified as homogenous catalyst, enzyme [3, 4] or heterogeneous catalyst, but conventional processing mostly involves an alkali catalyzed process. That the reason for base catalyzed process is less corrosive than the acid catalyzed and proceeds at higher rate [5]. However, when oil with high amounts of free fatty acid is used, these catalysts are not recommendable because of the soap formation. Thus, esterification process using strong acid catalyst has been shown to provide good conversion yield and high quality final product. Although the homogeneous catalyst for biodiesel production is relatively fast and high conversion with minimal side reactions, there are not very cost competitive with petrodiesel because the catalyst cannot be recovered and must be neutralized at the end of the reaction. Moreover, the processes are very sensitive to the presence of water and FFAs (Free Fatty Acids). In this work, focus on heterogeneous catalysts as bentonite clay that can be easily separated from product, reusable and low-cost catalyst. Raw bentonite clay was increased

acidity by ion-exchange from Na^+ to H^+ on the catalyst surface to provide high efficiency. The catalytic pelletize method was developed. The pellet bentonite clay was used as catalyst in a continuous packed bed reactor for esterification of free fatty acids (FFAs) in refined palm oil (RPO) and *Jatropha curcas* oil with methanol and ethanol.

1.2 Literature reviews

In 2009, Chongkhong *et al*. [6] investigated esterification of palm fatty acid distillate (PFAD) with methanol by using H_2SO_4 catalyst in a continuous process. Continuous production was compared to batch production at the same reaction condition, which a continuous process gave FAME 97.3% higher than bath process. The FFA in PFAD was reduced from 93 to less than 1.5 wt% in a continuous system. The optimum condition was obtained at mole ratio of methanol to PFAD to H_2SO_4 catalyst as 8.8:1:0.05, resident time of 60 min at 75°C.

In 2010, Zhang *et al*. [7] studied esterification of oleic acid in oil with methanol using H_2SO_4 catalyst in microstructured continuous reactor. The reported condition was 3 wt.% of H_2SO_4, methanol to oil mole ratio of 30, resident time 7 min, at 100°C, the acid value was reduced from 160 to 1.1 mg KOH/g (99% conversion).

Although homogeneous catalyst gave a high conversion but it caused problems in separation and catalyst recovery. Therefore, heterogeneous catalyst was more interesting. Park *et al*. [8] operated biodiesel production by esterification of vegetable oils with methanol using WO_3/ZrO_2 heterogeneous catalyst in a continuous process. In comparison, pellet-type catalyst contained lower pressure drop and weight loss than powder-type catalyst. Also, preparing of pellet-type WO_3/ZrO_2 catalyst was developed for using in the packed bed reactor. The pellet-type WO_3/ZrO_2 catalyst showed high activity about 70% conversion at optimum condition (mole ratio of oil to methanol as 1:19.4, temperature 75°C, 140 hours).

In 2007, Al-SBA-15 catalysts at ratio of Si/Al as 45, 136 and 215 were extruded by Murugesan *et al*. [9].The powdered materials were made into cylindrical

extrudates with the addition of bentonite as a binder. Extrusion composition was AlSBA-15: bentonite: methyl cellulose: H_2O as 14: 5: 6: 75 wt% for alkylation of phenol with *tert*-butanol. The surface area of the powder catalyst was around 950 m^2/g and that of extrudate was reduced close to 600 m^2/g. The optimum condition gave phenol conversion 62.9% and selective with para tertiary butylation using AlSBA-15 catalyst ratio of Si/Al as 45, temperature 200°C, weight hourly space velocity (WHSV) 1.5 $hour^{-1}$.

In 2008, Melero *et al*. [10] studied extrusion of Ti-SBA-15 as catalyst with bentonite clay as binding agent. The catalytic particle was tested activities in epoxidation of 1-octene with ethylbenzyl hydroperoxide in a continuous fixed bed reactor. The composition of pellet catalyst was ratio of Ti-SBA-15: bentonite: methyl cellulose as 60:40:5 wt%. The conversion of 1-octene was 68% at temperature 110°C, mole ratio of ethylbenzyl hydroperoxide with 1-octene as 0.12, flow rate of reactant 1.0 ml/min and reaction time 2 hours.

In 2008, Peng *et al*. [11] reported esterificaion of biodiesel production in batch reactor from waste oil feedstocks (50%) mixing with oleic acid (50%) which contained starting free fatty acid as 93% over heterogeneous acid catalyst comprising SO_4^{2-}/TiO_2-SiO_2 in a continuous system. The solid acid catalyst as SO_4^{2-}/TiO_2-SiO_2 can be recycled. The optimized reaction parameters are reaction temperature 200°C, mole ratio of methanol to oil 9:1 and catalyst concentration 3 wt%, 92% yield of methyl ester.

In 2010, Toshikuni *et al*. [12] studied esterification of oil with 14 wt% FFA with ethanol using cation-exchange resin as a catalyst in diameter of 11 mm for an expanded packed bed reactor. About 91% of FFA was converted to fatty acid ethyl ester (FAEE) mole ratio of ethanol to oil as 3.6:1, feed rate of reactant 0.10 cm^3/min at temperature 50°C. Amount of the cation-exchange resin packed catalyst was regulated in the range of 21.5-55.5 g by changing the column length between 30 and 75 cm.

In 2010, Pirola *et al*. [13] studied esterification of crude palm oil (FFA 6%) with methanol to give 44% FFA conversion using Amberlyst-46 as catalyst (7 g) in packed bed reactor (volume 0.5 L) with feed rate 10 ml/min, mole ratio of oil to methanol 1:6, resident time 30 min at temperature 65°C.

In 2011, Kusakabe *et al*. [14] investigated esterification of oleic acid with methanol in a three-phase fixed-bed reactor over Amberlyst-15 catalyst. The FAME yield was 97.5% when the methanol and oleic acid feed rates were 8.6 and 9.0 ml/h, a reaction temperature of 100°C in the fixed-bed (inner diameter as 16 mm, length as 200 mm) with a height of 5 cm.

Vijayakumar *et al*. [15] reported esterification of stearic acid with *p*-cresol over modified Indian bentonite clay catalysts for biodiesel production in batch reactor. The optimum condition of Acid Activated Indian Bentonite (AAIB) gave 96 % yield at mole ratio *p*-cresol to stearic acid 2:1, catalytic amount 0.5 g for 6 hours.

In 2009, Trabelsi *et al*. [16] investigated esterification of stearic, oleic and palmitic acids with short-chain alcohols (methanol, ethanol, propanol and butanol) using commercial clays in a semi-continuous reactor. The optimum condition of stearic acid (2 g) with 1-butanol (445 ml) provided 99.9% conversion using 0.2 g of montmorillonite KSF/0 clay as catalyst, feed rate of 1-butanol 0.02 mol/min at 150°C, during 4 hours.

1.3 Objectives

To investigate the optimum condition in esterification of FFA in refined palm oil (RPO) and *Jatropha curcas* oil with methanol and ethanol using pellet treated bentonite clay as catalyst in a continuous packed bed reactor.

1.4 Scopes of work

1. To modify bentonite clay as catalyst by ion-exchange method with H_2SO_4.
2. To characterize all prepared catalyst.
3. To study extrusion parameter and catalytic process.

4. To investigate the optimum conditions of FFA esterification by studying the effect of mole ratio of alcohol to oil, number of reactor, reaction temperature and catalyst amount.
5. To study the catalytic activity of reused catalyst.

CHAPTER II

THEORY

2.1 Biodiesel

Biodiesel, an alternative diesel fuel, is made from renewable biological sources such as vegetable oils and animal fats. It is biodegradable and nontoxic which has low emission profiles and so is environmentally beneficial. Biodiesel has been defined as the monoalkyl esters of long-chain fatty acids derived from renewable feedstocks, such as vegetable oils or animal fats, for used in compression-ignition (diesel) engines. The biodiesel that is considered as a possible substitute or extender of conventional diesel fuel is commonly composed of fatty acid methyl ester that are prepared from the triglycerides in vegetable oils by transesterification with methanol. The resulting biodiesel is quite similar to conventional diesel fuel in its main characteristics. Biodiesel is compatible with conventional diesel and both can be blended in any proportion. A number of plants are manufacturing biodiesel worldwide.

2.1.1 Advantages of biodiesel [17]

1. Conventional diesel engines can be operated without much, if any, modification on biodiesel.
2. Biodiesel can be used pure or in a mixture with hydrocarbon-based diesel fuels.
3. Biodiesel is nontoxic, safe of handle and biodegradable.
4. No evaporation of low-boiling components takes place.
5. Exhaust gas is free of SO_2 and halogens.
6. There is substantial reduction of soot, unburnt hydrocarbon, and also of carbon monoxide (when an oxidation catalyst is used) in the exhaust gases.
7. NO_X emissions increase slightly if there are no changes in the engine setting.

8. Good performance in auto-ignition of fatty esters results in a smooth running diesel engine.
9. Biodiesel consumption is similar to hydrocarbon-based diesel fuels.

2.1.2 Biodiesel property

Biodiesel is made up of fourteen different types of fatty acids, which are transformed into fatty acid methyl ester (FAME) by transesterification. Different fractions of each type of FAME present in various feedstocks influence some properties of fuels. Table 2.1 shows some of the properties defined in the ASTM standards for diesel and biodiesel. For Thailand, it has set legislative assembly characteristic and quality of biodiesel shown in Table 2.2.

Table 2.1 Comparison of fuel properties between diesel and biodiesel [18].

Fuel property	**Diesel**	**Biodiesel**
Fuel standard	ASTM D975	ASTM PS 121
Fuel composition	C10-C21 HC	C12-C22 FAME
Lower heating value, Btu/gal	131,295	117,093
Viscosity, @ 40°C	1.3-4.1	1.9-6.0
Specific gravity kg/l @ 60°F	0.85	0.88
Density, lb/gal @ 15°C	7.079	7.328
Water, ppm by wt	161	0.05% max
Carbon, wt %	87	77
Hydrogen, wt %	13	12
Oxygen, by dif. wt %	0	11
Sulfur, wt %	0.05 max	0.0-0.0024
Boiling point (°C)	188-343	182-338
Flash point (°C)	60-80	100-170
Cloud point (°C)	-15 to 5	-3 to 12
Pour point (°C)	-35 to -15	-15 to 10
Cetane number	40-55	48-65
Stoichiometric air/fuel ratio wt./wt.	15	13.8
BOCLE Scuff, grams	3,600	>7,000

Table 2.2 Characteristic and quality of biodiesel (methyl ester fatty acids) in Thailand [19].

Characteristic	**Value**	**Method of standard**
Methyl ester, %wt.	>96.5	EN 14103
Density at 15◦C, kg/m^3	860-900	ASTM D 1298
Viscosity at 40◦C, cSt	3.5-5.0	ASTM D 445
Flash point, ◦C	>120	ASTM D 93
Sulfur, %wt.	<0.0010	ASTM D2622
Carbon residue, on 10% distillation residue, wt%	<0.30	ASTM D 4530
Cetane number	>51	ASTM D 613
Sulfated ash, %wt.	<0.02	ASTM D 874
Water, %wt.	<0.050	ASTM D 2709
Total contaminate, %wt.	<0.0024	ASTM D 5452
Copper strip corrosion	<96.5	ASTM D 130
Oxidation stability at 110◦C, hours	>6	EN 14112
Acid value, mg KOH/g	<0.50	ASTM D 664
Iodine value, g Iodine/100 g	<120	EN 14111
Linolenic acid methyl ester, %wt.	<12.0	EN 14103
Methanol, %wt.	<0.20	EN 14110
Monoglyceride, %wt.	<0.80	EN 14105
Diglyceride, %wt.	<0.20	EN 14105
Triglyceride, %wt.	<0.20	EN 14105
Free glycerin, %wt.	<0.02	EN 14105
Total glycerin, %wt.	<0.25	EN 14105

2.2 The production of biodiesel [20]

2.2.1 Direct use and blending

In 1980, Bartholomew addressed the concept of using food for fuel. It was not practical to substitute 100% vegetable oil for diesel fuel. But a blend of 20% vegetable oil and 80% diesel fuel was successful. Mixture of degummed soybean oil and No. 2 diesel fuel in the ratio of 1:2 and 1:1 were tested for engine performance, the results indicated that 1:2 blend should be suitable as a fuel for agricultural. Two problems associated with the use of vegetable oil as fuels were oil deterioration and incomplete combustion.

2.2.2 Thermal cracking (pyrolysis)

To solve the problem of high viscosity of vegetable oils, the pyrolysis was chosen to produce the biodiesel. The pyrolysed material can be vegetable oils, animal fat, natural fatty acids and methyl ester of fatty acids. A large scale of thermal cracking of tung oil calcium soaps was reported. Tung oil was first saponified with lime and then thermally cracked to yield a crude oil, which was refined to produce diesel fuel. Soybean oil was thermally decomposed and distilled in air and nitrogen sparged with a standard ASTM distillation apparatus. Moreover, Rapeseed oil was pyrolysed to produce a mixture of methyl esters in the tubular reactor between 500 and 850°C in nitrogen. The mechanism of thermal decomposition of triglycerides was shown in Figure 2.1.

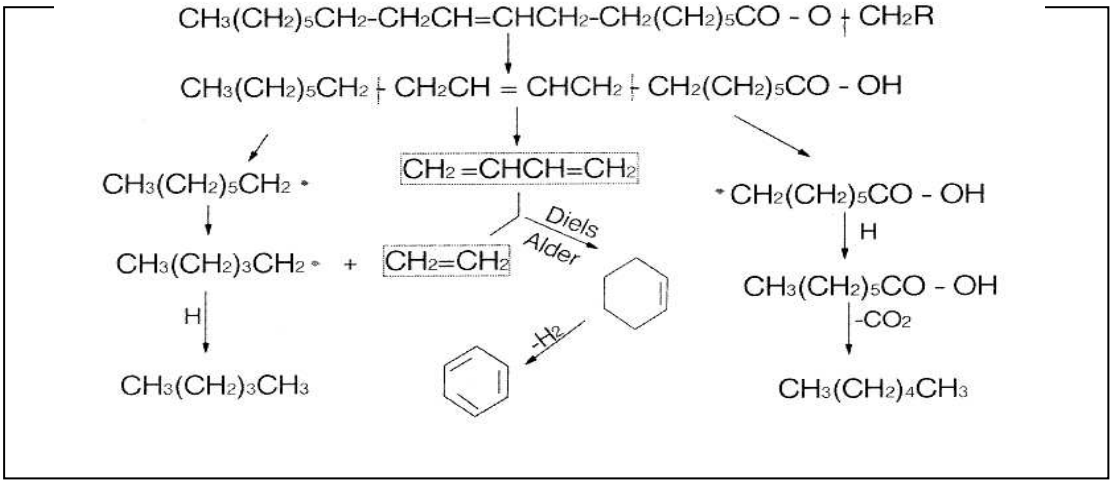

Figure 2.1 The mechanism of thermal decomposition of triglycerides.

2.2.3 Transesterification

Transesterification is the displacement of alcohol from ester by another in a process similar to hydrolysis, except than alcohol is used instead of water. A catalyst is usually used to improve the reaction rate and yield. Because the reaction is reversible, excess alcohol is used in shifting the equilibrium to the product side. The reaction can be catalyzed by alkali, acid or enzyme such as NaOH, KOH, H_2SO_4 and lipase, respectively. The transesterification reaction diagram of triglycerides is presented in the Figure 2.2.

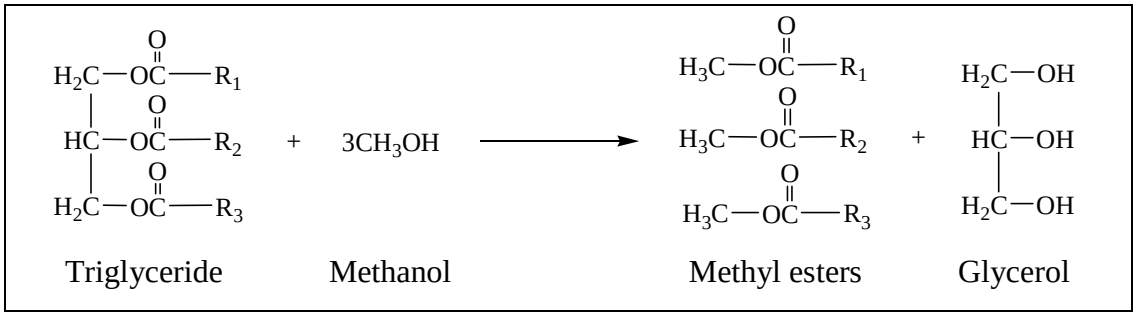

Figure 2.2 Typical transesterfication diagram of triglyceride.

2.2.3.1 Transesterification kinetics and mechanism [21]

Transesterification of triglycerides (TGs) with alcohol proceeds via three consecutive and reversible reactions where the FFA ligands combine with alcohol to produce a fatty acid alkyl ester, diglyceride and monoglyceride intermediates, and finally glycerol by-product. The stoichiometric reaction requires 1 moles of TG and 3 mole of methanol to produce 3 mole of linear ester and 1 mole of glycerol. In presence of excess alcohol, the forward reaction is pseudo-first order and the reverse reaction is found to be second-order. It was observed that transesterification is faster when catalyzed by alkali. The mechanism of acid and alkali-catalyzed transesterification is described in Figures 2.3 and 2.4, respectively.

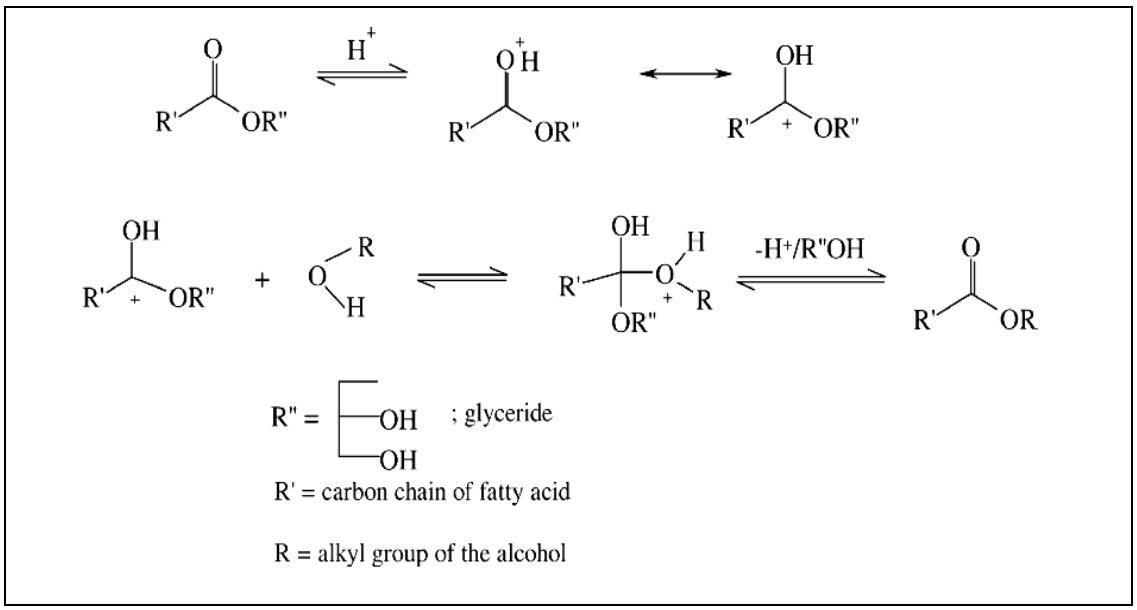

Figure 2.3 Mechanism of acid catalyzed transesterification reaction.

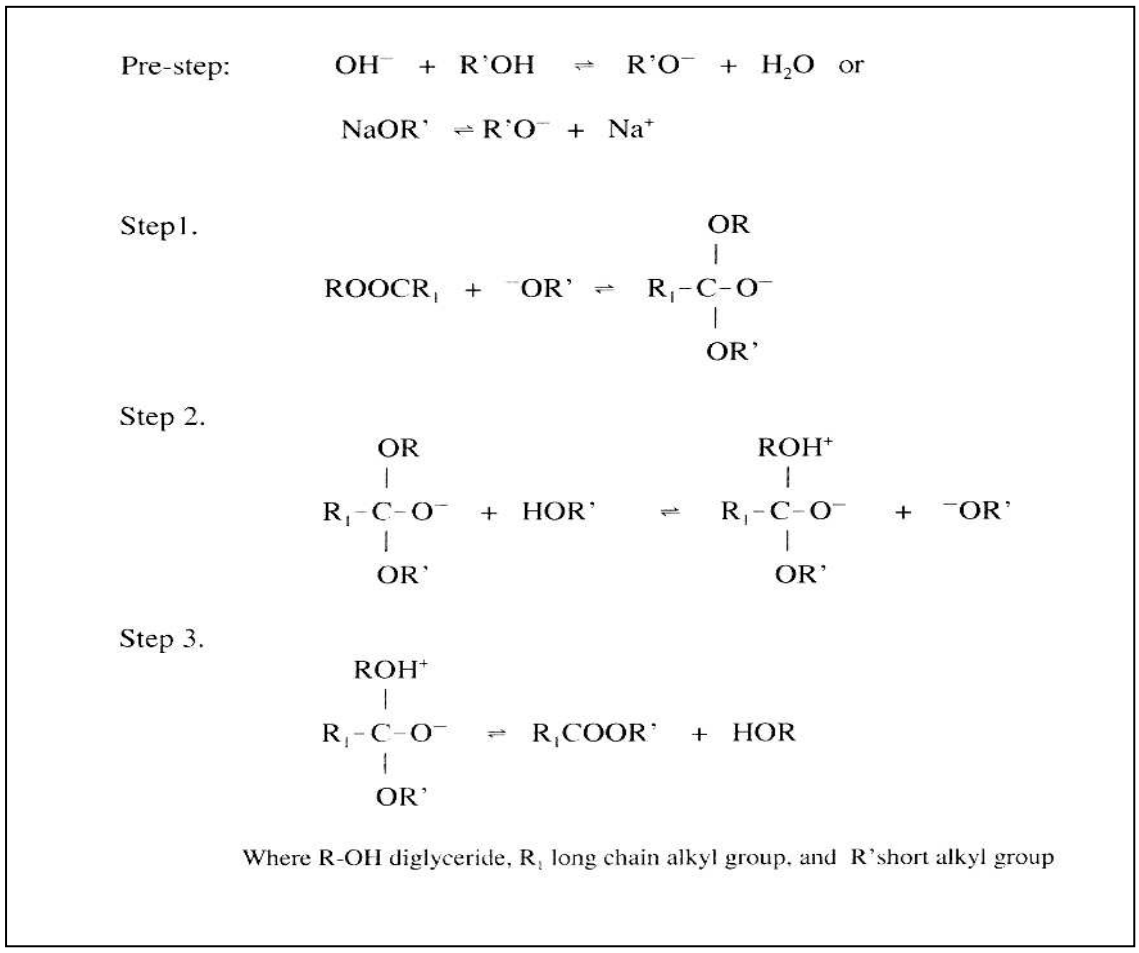

Figure 2.4 Mechanism of base catalyzed transesterification reaction.

2.2.4 Esterificaton

Esterificaton is the chemical process for making ester, which are compounds for the chemical structure R-COOR', where R and R' are either alkyl or aryl groups. The most common method for preparing esters is to heat a carboxylic acid or free fatty acid with an alcohol, while removing the water that is formed. Esterification is among the simplest and most often performed organic transformation. The esterification reaction diagram of free fatty acid is shown in the Figure 2.5. The mechanism of acid and alkali catalyzed esterifications are presented in Figure 2.6 and 2.7, recpectively.

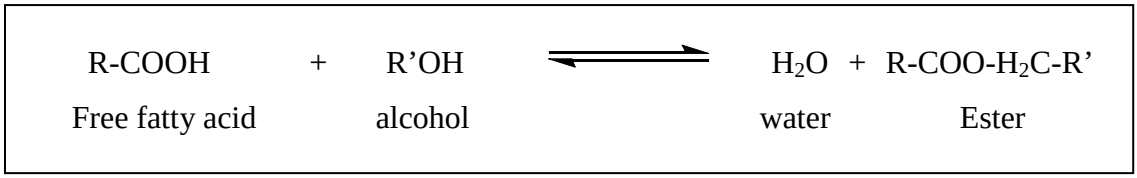

Figure 2.5 Typical esterification diagram of free fatty acid.

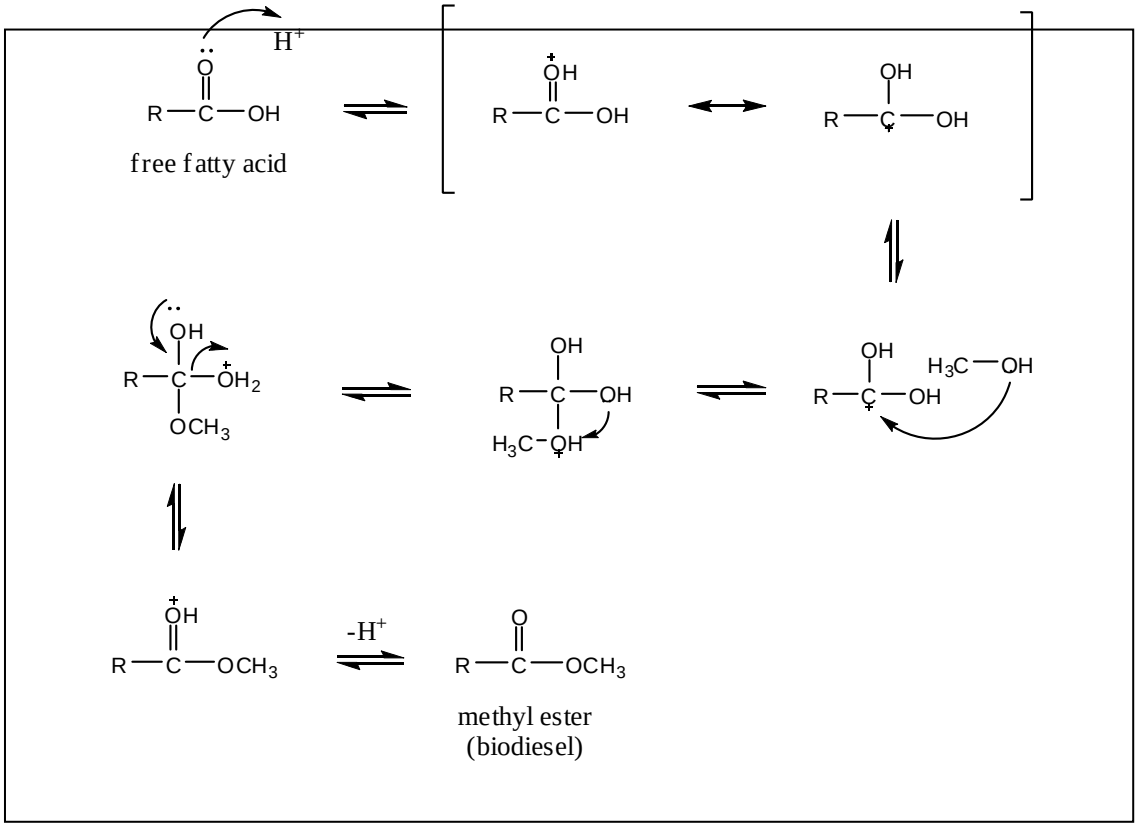

Figure 2.6 Mechanism of acid catalyzed esterification of free fatty acid.

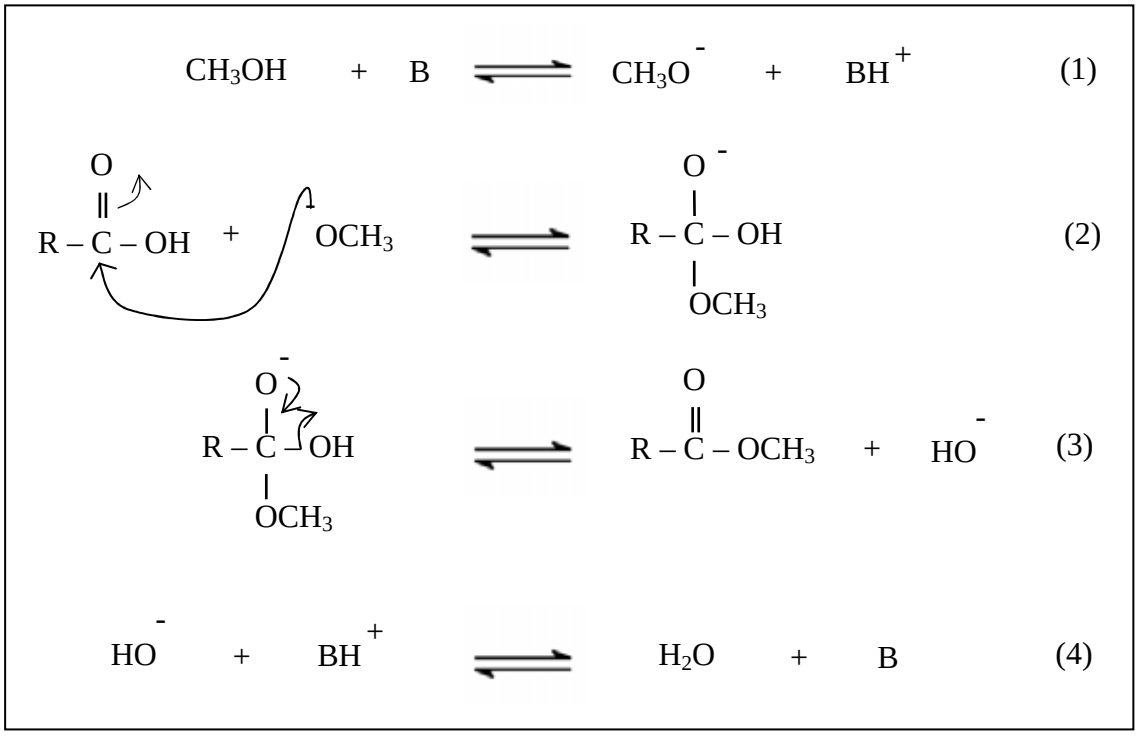

Figure 2.7 Mechanism of base catalyzed esterification of free fatty acid.

2.3 Free fatty acids (FFAs) [22]

Fatty acids are aliphatic monocarboxylic acids derived from or contained in esterified form in an animal or vegetable fat, oil or wax. Natural fatty acids commonly have a chain of 4 to 28 carbons, which may be saturated or unsaturated. By extension, the term is sometimes used to embrace all acyclic aliphatic carboxylic acids.

2.3.1 Types of fatty acid

2.3.1.1 Saturated fatty acids

Saturated fatty acids do not contain any double bonds. The term saturated refers to hydrogen, in that all carbons contain (apart from the carboxylic acid group) as many hydrogens as possible. Each carbon within the chain contains 2 hydrogen atoms. The saturated fatty acids are shown in Table 2.3.

Table 2.3 Saturated fatty acids.

Common name	IUPAC name	Chemical structure	C no. : db
Lauric	Dodecanoic acid	$CH_3(CH_2)_{10}COOH$	C12:0
Myristic	Tetradecanoic acid	$CH_3(CH_2)_{12}COOH$	C14:0
Palmitic	Hexadecanoic acid	$CH_3(CH_2)_{14}COOH$	C16:0
Stearic	Octadecanoic acid	$CH_3(CH_2)_{16}COOH$	C18:0

2.3.1.2 Unsaturated fatty acids

Unsaturated fatty acids are of similar form, except that one or more alkenyl functional groups exist along the chain, with each alkene substituting a single-bonded part of the chain with a double-bonded portion. The two next carbon atoms in the chain that are bound to either side of the double bond can occur in a *cis* or *trans* configurations, its were shown in Figure 2.8. Examples of unsaturated fatty acids were presented in Table 2.4. [23]

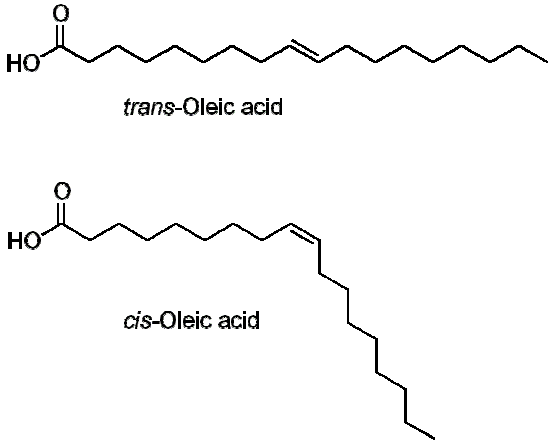

Figure 2.8 Comparison of the *trans* isomer and the *cis*-isomer of oleic acid.

Table 2.4 Unsaturated fatty acids.

Common name	Chemical structure	C no. : db
Myristoleic acid	$CH_3(CH_2)_3CH=CH(CH_2)_7COOH$	C14:1
Palmitoleic acid	$CH_3(CH_2)_5CH=CH(CH_2)_7COOH$	C16:1
Oleic acid	$CH_3(CH_2)_7CH=CH(CH_2)_7COOH$	C18:1
Linoleic acid	$CH_3(CH_2)_4CH=CHCH_2CH=CH(CH_2)_7COOH$	C18:2

2.3.2 Palmitic acid

Palmitic acid is one of the most common saturated fatty acids found in animals and plants. It has the formula $C_{16}H_{32}O_2$ and is a major component of the oil from palm trees (palm oil and palm kernel oil). Palmitic acid was discovered by Edmond Frémy in 1840, in saponified palm oil and is the first fatty acid produced during lipogenesis (fatty acid synthesis) and from which longer fatty acids can be produced. Palmitate negatively feeds back on acetyl-CoA carboxylase (ACC) which is responsible for converting acetyl-ACP to malonyl-ACP on the growing acyl chain, thus preventing further palmitate generation.

2.3.3 Oleic acid

Oleic acid is a monounsaturated omega-9 fatty acid found in various animal and vegetable sources. It has the formula $C_{18}H_{34}O_2$. The saturated form of this acid is stearic acid. Oleic acid makes up 55-80% of olive oil, 40-50% of palm oil and 15-20% of grape seed oil.

2.3.4 Linoleic acid

Linoleic acid is an unsaturated omega-6 fatty acid. It is a colorless liquid. In physiological literature, it is called 18:2(n-6). Chemically, linoleic acid is a carboxylic acid with an 18-carbon chain and two *cis* double bonds; the first double bond is located at the sixth carbon from the omega end. It is found in the lipids of cell

membranes. It is abundant in many vegetable oils, especially safflower and sunflower oils.

2.3.5 Fatty acids composition of palm oil

The fatty acids of palm oil could be of the same type or different. The property of a triglyceride will depend on the different fatty acids that combine to form the triglyceride. The fatty acids themselves are different depending on their chain length and degree of saturation. The short chain fatty acids are of lower melting point and are more soluble in water. Whereas, the longer chain fatty acids have higher melting points. The melting point is also dependent on degree of non-saturation. Unsaturated acids will have a lower melting point compared to saturated fatty acids of similar chain length. The two most predominant fatty acids in palm oil are C18:1 (unsaturated) oleic acid and C16:0 (saturated) palmitic acid. Typical fatty acid composition of palm oil is given in Table 2.5.

Table 2.5 Typical free fatty acid composition in palm oil.

Fatty acid	**C no. : db**	**% wt**
Oleic acid	C18 : 1	45.22
Palmitic acid	C16 : 0	37.94
Linoleic acid	C18 : 2	10.89
Stearic acid	C18 : 0	3.84
Myristic acid	C14 : 0	1.19
Lauric acid	C12 : 0	0.67
Linolenic acid	C18 : 3	0.25

C: carbon, DB: double bond

2.4 ***Jatropha curcas Linn.*** [24, 25, 26]

*Jatropha curcas Linn.*was a native tropical plant of America and carried out tropical and subtropical parts of Asia and Africa. There is one family with rubber and cassava which can grow quickly in a less fertile and non-fertile land due to requires low water. In Thailand, *Jatropha curcas Linn.* is called “Saboo Dam” which is found near the rice fields as the farmers planted them and using them as herb. *Jatropha curcas* seed has rich oil yield of 25 to 45 percent by weight. Their leaves also yield a dye and latex which has many medicinal uses that could support potential pharmaceutical industries. *Jatropha curcas Linn.* was a non–edible oil that approved as a good feedstock for biodiesel.

Figure 2.9 *Jatropha curcas Linn.*

Table 2.6 Problems in use of *Jatropha curcas* oil as fuel in diesel engine.

Problems	Causes
Coking of injectors on piston and head of engine	High viscosity of raw oil, incomplete combustion of fuel. Poor combustion at part load with raw oil
Carbon deposits on piston and head of engine	High viscosity of oil, incomplete combustion of fuel.
Excessive engine wear	High viscosity of raw oil, incomplete combustion of fuel. Dilution of engine lubricating oil due to blow-by of raw oil

The above problems can be solved by converting raw jatropha oil in to biodiesel through transesterification or esterification process which involves making the triglycerides or free fatty acids of jatropha oil to react with alcohol over acid-basic catalyst.

2.5 Type of the catalysts [27]

Catalysts can be divided into two main types, heterogeneous and homogeneous catalysts. Biocatalyst is often seen as a separate group. In nature enzymes are catalyst in metabolic pathway whereas in biocatalysts enzymes are used as catalyst in organic chemistry. Heterogeneous catalyst is present in different phases from the reactants. Whereas, homogeneous catalyst is in the same phase.

2.5.1 Homogeneous catalysts

Homogeneous catalysts are in the same phase as the reactants. The catalyst is a molecule which facilitates the reaction. The catalyst initiates reaction with one or more reactants to form intermediate and in some cases one or more products. Subsequent steps lead to the formation of remaining products and to the regeneration of the catalyst. Typically, everything will be presence as gas or contained in a single liquid phase. In addition, the catalysis of organic reactions by metal complexes in solution has grown rapidly in both scientific and industrial importance.

2.5.2 Heterogeneous catalysts

Heterogeneous catalyst is presented in different phases from the reactants e.g. a solid catalyst in a liquid reaction mixture. A simple model heterogeneous catalysis involves the catalyst providing a surface on which the reactants temporarily become adsorbed. Bonds in the reactants become weakened sufficiently for new bonds to be created. The bonds between the products and the catalyst are weaker, so the products are released. The mechanism of heterogeneous catalysis comprises five steps between compounds adsorbed on the surface of solid catalyst [28].

(1) Diffusion of the reacting substances over the catalyst particle.
(2) Adsorption of the reacting substances on the catalyst.
(3) Interaction of the reacting substances on the surface of catalyst.
(4) Desorption of the reaction products from the catalyst particle.
(5) Diffusion of the reaction products into the surrounding medium.

Furthermore, catalyst particles have internal pores that are accessible to the reactant molecules, so that diffusion proceeds in two steps, external and internal surface.

2.6 **Bentonite clay** [29, 30]

Bentonite minerals is an aluminium phyllosilicate which impure clay consisting mostly of montmorillonite. Bentonite normally forms from weathering of volcanic ash, most often in the presence of water.The properties of bentonite are an ability to form thixotrophic gels with water that ability to absorb large quantities of water to increase volume of as much as 12–15 times of dry volume, and a high cation exchange capacity. There are different types of bentonite, dominant element, such as sodium (Na^+), calcium (Ca^{2+}) and potassium (K^+). Sodium and calcium bentonite was used base industrial material. It is therefore a mixture of minerals. No “molecular” formula can be given.

The most important bentonite clay is the montmorillonite group of minerals. Figure 2.10, montmorillonite feature the layered sheet structural that is typical of most minerals. Each sheet consists of a three-layer sandwich of ions in octahedral form.

The central layer consists of aluminum ions surrounded by oxygen ions in octahedral form. The outer layers are silicon ions surrounded oxygen ions in tetrahedral form [31]. The chemical formula for montmorillonite is usually given as $(OH)_4Al_4Si_8O_{20}.nH_2O$.

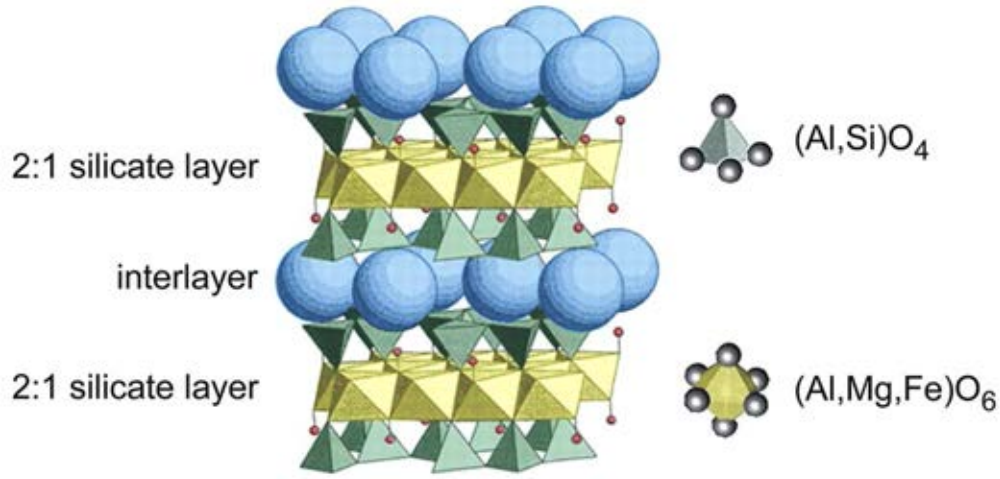

Figure 2.10 Structure of montmorillonite.

2.6.1 Types of bentonite [32]

2.6.1.1 Sodium bentonite

Sodium bentonite expands when wet, absorbing as much as several times its dry mass in water. Because of its excellent colloidal properties, it is often used in drilling mud for oil and gas wells and for geotechnical and environmental investigations. The property of swelling also makes sodium bentonite useful as a sealant, especially for the sealing of subsurface disposal systems for spent nuclear fuel and for quarantining metal pollutants of groundwater. Similar uses include making slurry walls, waterproofing of below-grade walls, and forming other impermeable barriers. It is also used to form a barrier around newly planted trees to constrain root growth so as to prevent damage to nearby pipes, footpaths and other infrastructure. Various surface modifications to sodium bentonite improve some rheological or sealing performance in geoenviromental applications, for example, the addition of polymers.

2.6.1.2 Calcium bentonite

Calcium bentonite is a useful adsorbent of ions in solution, as well as fats and oils, being a main active ingredient of fuller's earth, probably one of the earliest industrial cleaning agents. Calcium bentonite may be converted to sodium bentonite (termed sodium beneficiation or sodium activation) to exhibit many of sodium bentonite's properties by a process known as "ion exchange". In common usage, this means adding 5–10% of a soluble sodium salt such as sodium carbonate to wet bentonite, mixing well, and allowing time for the ion exchange to take place and water to remove the exchanged calcium. Some properties, such as viscosity and fluid loss of suspensions, of sodium-beneficiated calcium bentonite (or sodium-activated bentonite) may not be fully equivalent to those of natural sodium bentonite.

2.7 Modification of clay

2.7.1 Ion exchange [34]

Ion exchange is an exchange of ions between two electrolytes or between an electrolyte solution and a complex. For a cation-exchanging clay, e.g., a montmorillonite, *M*, one can write:

$$MA + B^{+} \leftrightarrow MB + A^{+} \qquad (2.1)$$

where A^{+} and B^{+} are cations. The montmorillonite can be used as a cation exchanger in any of the forms, *MA*, *MB*, etc. In the chemical industry, as well as for purposes of water-softening, very extensive use is made of ion exchange reactions. However, in most cases, one uses synthetic organic ion exchange materials, such as, typically, sulfonated polystyrene, as a cation exchanger. For water softening, i.e., the removal of Ca^{2+} from "hard" water one uses a cation exchanger, *X*, in the sodium form:

$$2XNa + Ca^{2+} \leftrightarrow XCa + 2Na^{+} \qquad (2.2)$$

For agricultural applications mineral (clay) ion exchangers remain important. The cation exchanging properties of, e.g., montmorillonites are also useful for binding organic cations. One example of this is the binding of alkaloids (which are positively charged), and thus as an antidote for a variety of poisons, which often are of alkaloid nature. For the relatively minor influence of different exchanged cations on the surface properties of various ion exchanged clays. The binding of cation exchanging montmorillonites to alkyl amines is important in the formation of bentones, which are used, e.g., in gel formation of oil and petroleum products.

2.8 Characterization of catalysts structure

2.8.1 Powder x-ray diffraction (XRD) [35]

X-ray powder diffraction (XRD) is a reliable technique that can be used to identify mesoporous structure. Typically, the XRD pattern of hexagonal symmetry show five well-resolved peaks that can be indexed to the corresponding lattice planes of Miller indices (100), (110), (200), (210), and (300). These XRD peaks appear at small angle (2θ angle between 2 and 5 degree) due to the materials are not crystalline at atomic level, diffraction at higher angles are not observed.

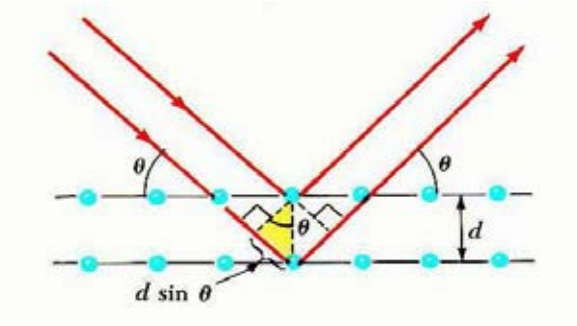

Figure 2.11 Diffraction of X-ray by regular planes of atoms.

Figure 2.11 shows a monochromatic beam of X-ray incident on the surface of crystal at an angle, θ. The scattered intensity can be measured as a function of scattering angle 2θ. The resulting XRD pattern efficiently determines the different phases present in the sample structure. Using this method, Bragg's law is able to

determine the interplanar spacing of the samples, from diffraction peak according to Bragg's angle.

$$n\lambda = 2d \sin\theta$$

Where the integer *n* is the order of the diffracted beam, λ is the wavelength; *d* is the interplanar distance of the crystal (the *d*-spacings) and θ is the angle of between the incident beam and these planes.

2.8.2 **Nitrogen adsorption-desorption technique** [36, 37]

The N_2 adsorption-desorption technique is used to determine the physical properties that are surface area, pore volume, pore diameter and pore-size distribution of solid catalysts. Adsorption of gas by a porous material is described by an adsorption isotherm, the amount of adsorbed gas by the material at a fixed temperature as a function of pressure. Porous materials are frequently characterized in terms of pore sizes derived from gas sorption data. The IUPAC classification of adsorption isotherms is illustrated in Figure 2.12.

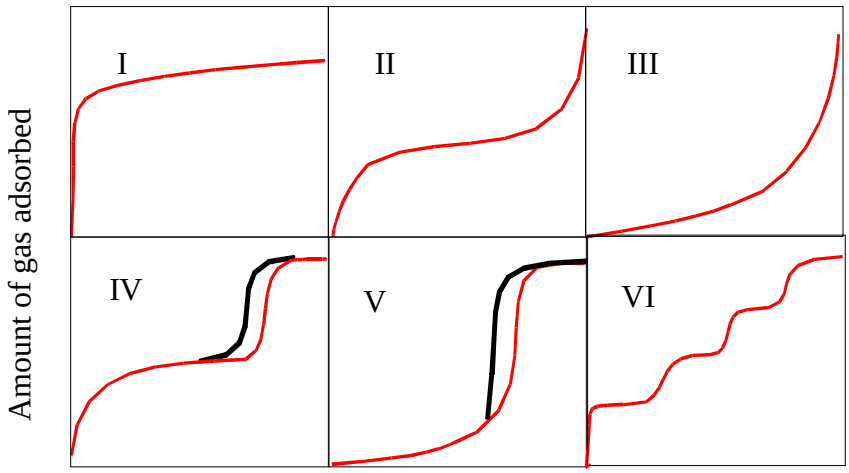

Figure 2.12 The IUPAC classification of adsorption isotherm.

Adsorption isotherms are described as shown in Table 2.7 based on the strength of the interaction between the sample surface and adsorptive. Pore size distribution is measured by the use of nitrogen adsorption/desorption isotherm at liquid nitrogen temperature and relative pressures (P/P_o) ranging from 0.05-0.1. The large uptake of nitrogen at low P/P_o indicates filling of the micropores (<20 Å) in the adsorbent. The linear portion of the curve represents multilayer adsorption of nitrogen on the surface of the sample, and the concave upward portion of the curve represents filling of mesoporous and macropores. The multipoint Brunauer, Emmett and Teller (BET) method is commonly used to measure total surface area.

$$\frac{1}{W[(P_o/P)-1]} = \frac{1}{W_m C} + \frac{C-1}{W_m C}(P/P_o)$$

where W is the weight of nitrogen adsorbed at a given P/P_o, and W_m is the weight of gas to give monolayer coverage, and C is a constant that is related to the heat of adsorption. A slope and intercept are used to determine the quantity of nitrogen adsorbed in the monolayer and calculate the surface area. For a single point method, the intercept is taken as zero or a small positive value, and the slope from the BET plot is used to calculate the surface area. The surface area reported depend upon the method used, as well as the partial pressures at which the data are collected.

\

Table 2.7 Features of adsorption isotherms.

Type	Interaction between sample surface and gas adsorbate	Porosity	Example of sample-adsorbate
I	relatively strong	Micropores	activated carbon-N_2
II	relatively strong	Non porous	oxide-N_2
III	weak	Non porous	carbon-water vapor
IV	relatively strong	Mesopore	silica-N_2
V	weak	Micropores Mesopore	activated carbon-water vapor
VI	relatively strong sample surface has an even distribution of energy	Nonporous	graphite-Kr

2.8.3 Scanning electron microscope [38]

The scanning electron microscope (SEM) has unique capabilities for analyzing surfaces and morphology of materials. It is analogous to the optical microscope, although different radiation sources serve to produce the required illumination. Whereas the optical microscope forms an image from light reflected from a sample surface, the SEM uses electrons for image formation. The different wavelength of these radiation sources result in different resolution levels: electron have much shorter wavelength than light photons, and shorter wavelength are capable of generating the higher resolution information. Enhanced resolution in turn permits higher magnification without loss of detail. The maximum magnification of the light microscope is about 2,000 times; beyond this level is “empty magnification”, or the point where increased magnification does not provide additional information. This upper magnification limit is a function of the wavelength of visible light, 2000 Å, which equal the theoretical maximum resolution of conventional light microscope. In comparison, the wavelength of electron is less than 0.5 Å, and theoretically the

maximum magnification of electron beam instrument is beyond 800,000 times. Because of instrumental parameters, practical magnification and resolution limits are about 75,000 times and 40 Å in a conventional SEM. The SEM consists basically of four systems:

1. The *illuminating/imaging system* produces the electron beam and directs it onto the sample.
2. The *information system* includes the data released by the sample during electron bombardment and detectors which discriminate among analyze these information signals.
3. The *display system* consists of one or two cathode-ray tubes for observing and photographing the surface of interest.
4. The *vacuum system* removes gases from the microscope column which increase the mean free path of electron, hence the better image quality.

2.8.4 X-ray Fluorescence (XRF) [39]

An electron can be ejected from its atomic orbital by the absorption of a light wave (photon) of sufficient energy. The energy of the photon (hv) must be greater than the energy with which the electron is bound to the nucleus of the atom. When an inner orbital electron is ejected from an atom, an electron from a higher energy level orbital will be transferred to the lower energy level orbital. During this transition a photon maybe emitted from the atom. This fluorescent light is called the characteristic X-ray of the element. The energy of the emitted photon will be equal to the difference in energies between the two orbitals occupied by the electron making the transition. Because the energy difference between two specific orbital shells, in a given element, is always the same (i.e. characteristic of a particular element), the photon emitted when an electron moves between these two levels, will always have the same energy. Therefore, by determining the energy (wavelength) of the X-ray light (photon) emitted by a particular element, it is possible to determine the identity of that element.

For a particular energy (wavelength) of fluorescent light emitted by an element, the number of photons per unit time (generally referred to as peak intensity or count rate) is related to the amount of that analyst in the sample. The counting rates for all detectable elements within a sample are usually calculated by counting, for a set amount of time, the number of photons that are detected for the various analyst characteristic X-ray energy lines. It is important to note that these fluorescent lines are actually observed as peaks with a semi-Gaussian distribution because of the imperfect resolution of modern detector technology. Therefore, by determining the energy of the X-ray peaks in a sample's spectrum, and by calculating the count rate of the various elemental peaks, it is possible to qualitatively establish the elemental composition of the samples and to quantitatively measure the concentration of these elements.

2.8.5 Thermogravimetric Analysis (TGA) [40, 41]

TGA was used primarily for determining thermal stability of polymers. The most widely used TGA method is based on measurement of weight on a sensitive balance (called a *thermobalance*) as sample temperature was increased in air or in an inert atmosphere. This is referred to as *nonisothermal TGA.* Data are recorded as a thermogram of weight versus temperature. Weight loss may arise from evaporation of residual moisture or solvent, but at higher temperatures it results from polymer decomposition. Besides providing information on thermal stability, TGA may be used to characterize polymers through loss of a known entity, such as HCl from poly(vinyl chloride). Thus weight loss can be correlated with percent vinyl chloride in a copolymer. TGA is also useful for determining volatilities of plasticizers and other additives. Thermal stability studies are the major application of TGA. A method known as hi-resolution TGA is often employed to obtain greater accuracy in areas where the derivative curve peaks.

A variation of the method is to record weight loss with time at a constant temperature. Called *isothermal TGA,* this is less commonly used than nonisothermal TGA. Modern TGA instruments allow thermograms to be recorded on microgram quantities of material. Some instruments are designed to record and

process DSC and TGA data simultaneously, and may also be adapted for gas chromatographic and or mass spectrometric analysis of effluent degradation products.

2.9 Reactor geometry [42]

The reactors used for established processes are usually complex designs which have been developed and evolved over a period of years to suit the requirements of the process, and are unique designs. However, it is convenient to classify reactor designs into the following broad categories.

2.9.1 Stirred tank reactors

Stirred tank agitated reactors consist of a tank fitted with a mechanical agitator and a cooling jacket or coils. They are operated as batch reactors or continuous reactors. Several reactors may be used in series.

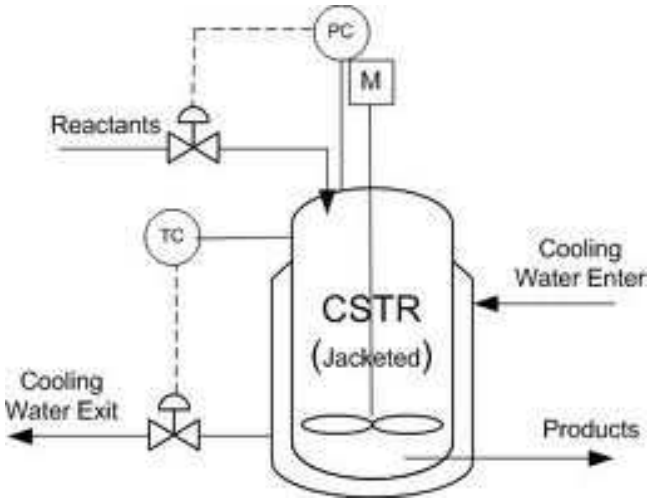

Figure 2.13 Continuous stirred tank reactor (CSTR).

The *stirred tank reactor* can be considered the basic chemical reactor modeling on a large scale the conventional laboratory flask. Tank sizes range from a few litres to several thousand liters. They are used for homogeneous and heterogeneous liquid-liquid and liquid-gas reactions and for reactions that involve freely suspended solids, which are held in suspension by the agitation. As the degree

of agitation is under the designers control, stirred tank reactors are particularly suitable for reactions where good mass transfer or heat transfer is required.

2.9.2 Tubular reactors

Tubular reactors are generally used for gaseous reactions, but are also suitable for some liquid phase reactions. If high heat transfer rates are required small diameter tubes are used to increase the surface area to volume ratio. Several tubes may be arranged in parallel, connected to a manifold or fitted into a tube sheet in a similar arrangement to a shell and tube heat exchangers. For high temperature reactions the tubes may be arranged in a furnace.

2.9.3 Packed bed reactors

There are two basic types of packed bed reactor, those in which the solid is a reactant and those in which the solid is a catalyst. In chemical process industries, the emphasize is mainly on the designing of catalytic reactors. Industrial packed bed catalytic reactors range in size from small tubes, a few centimeters diameter to large diameter packed beds. Packed-bed reactors are used for gas and gas-liquid reactions. Heat-transfer rates in large diameter packed beds are poor therefore where high heat-transfer rates are required, fluidised beds should be considered.

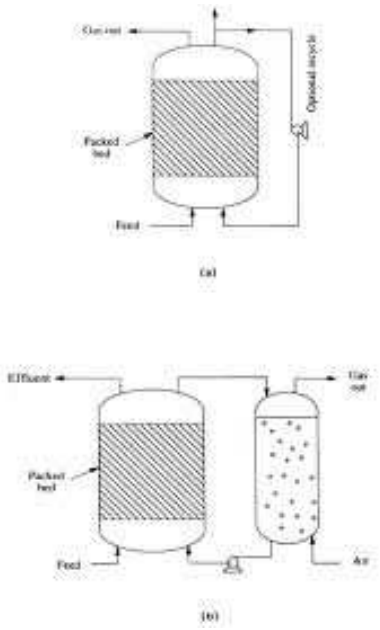

Figure 2.14 Packed bed reactors.

2.9.4 Fluidised bed reactors

A fluidized-bed reactor (Figure 2.16) is a combination of the two most common, packed-bed and stirred tank, continuous flow reactors. It is very important to chemical engineering because of its excellent heat and mass transfer characteristics. The essential features of a fluidized bed reactor are that the solids are held in suspension by the upward flow of the reacting fluid. This promotes high mass and heat transfer rates and good mixing. The principal advantage of a fluidized bed over a fixed bed is the higher heat transfer rate, fluidized beds are also useful where it is necessary to transport large quantities of solids as part of the reaction processes. Fluidization can only be used with relatively small a sized particle that is less than 300μm. This is the limitation of the process.

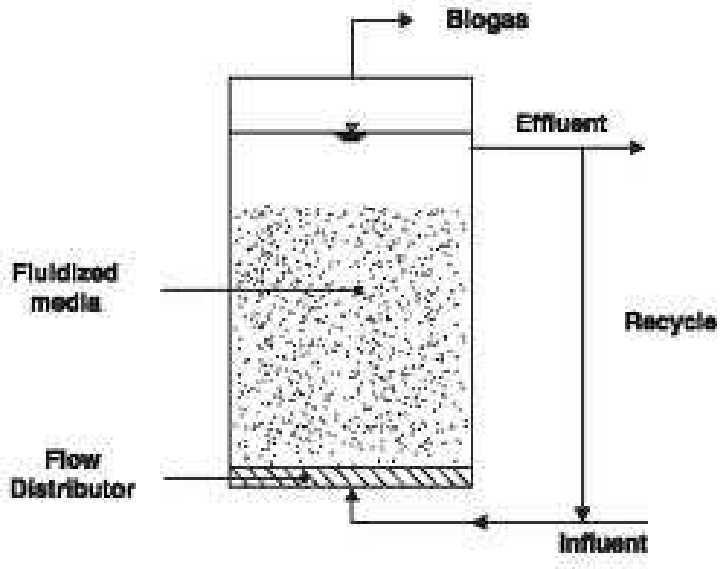

Figure 2.15 Fluidized bed reactors.

CHAPTER III
EXPERIMENTAL

3.1 Instruments, apparatus and analytical techniques

3.1.1 X-ray fluorescence spectroscopy (XRF)

The elemental analysis of the catalysts were analyzed using the Oxford ED-2000 X-ray Fluorescence Spectrometer at the Scientific and Technological Research Equipment Centre of Chulalongkorn University.

3.1.2 Powder X-ray diffraction (XRD)

The XRD pattern and d-spacing of raw bentonite (Na^+ form) and dried treated bentonite with 0.5 M H_2SO_4 were determined by a Rigaku, Dmax 2200/Ultima$^+$ diffractometer equipped with a monochromator and Cu Kα radiation. The tube voltage and current were set at 40 kV and 30 mA, respectively. The diffraction pattern was recorded in the 2-theta ranged from 2 to 50 degree with scan speed of 3 degree/min and scan step of 0.02 degree. The scattering slit, divergent slit and receiving slit were fixed at 0.5 degree, 0.5 degree and 0.15 mm, respectively.

3.1.3 Infrared spectroscopy (IR spectroscopy)

Attenuated Total Reflection Infrared (ATR-IR) spectra were performed on a Perkin-Elmer (Spectrum One). ATR-IR spectroscopy technique was used to analyze functional group. It was also suitable for characterization of material which was either too thick or too strong absorbing to be analyzed by transmission.

3.1.4 Scanning electron microscopy (SEM)

The morphology and size of raw bentonite (Na^+ form) and treated bentonite particles were identified by a JSM-5410 LV scanning electron microscopy (SEM). In SEM analysis, the samples were coated with gold.

3.1.5 N_2- adsorption/desorption

N_2 adsorption-desorption isotherms, BET specific surface area, and pore size distribution of the catalysts were carried out using a BEL Japan, BELSORP-mini instrument. The pure materials were weighted nearly 40 mg and weighted exactly after pretreated at 400^{o}C for 3 hrs. The functionalized materials were pretreated at 150^{o}C for 3 hrs before each measurement.

3.1.6 Thermogravimetric analysis (TGA)

Thermal stability and weight loss of treated bentonite were analyzed using TGA Netzsch 5 under N_2 gas, heating rate 10°C/min at Scientific and Technological Research Equipment Centre of Chulalongkorn University.

3.1.7 Potentiometric titration

Free fatty acid (FFA, as oleic acid) was analyzed by potentiometric titration (Mettler Toledo T50). Approximately 1.0 g of oil sample with 50 ml of ethanol was titrated with 0.25 M NaOH in ethanol by using phenolphthalein as indicator (Modified from ASTM D 5555-95 (Reapproved 2006)).

Figure 3.1 Potentiometric measurement.

3.1.8 Glass column reactor

Esterification reaction of free fatty acid was performed in a glass column reactor, diameter as 10 mm, length as 33.5 cm and filter length at bottom of reactor as 3.5 cm.

3.2 Chemicals

1. Oleic acid, $C_{18}H_{34}O_2$ (Aldrich, 90%)
2. Methanol, CH_3OH (Merck, 99.9%)
3. Ethanol, CH_3CH_2OH (Merck, 99.9%)
4. Sulfuric acid, H_2SO_4 (Merck, 95-97%)
5. Sodium hydroxide, NaOH (Merck, 99%)
6. Potassium hydroxide, KOH (BDH, ≥85%)
7. Bentonite clay (Siam volclay, Na^+ from)
8. Refined palm olein cooking oil (Oleen brand)
9. *Jatropha curcas* oil (PTT research and technology institute)
10. Acetone, C_3H_6O (Merck, 99.5%)
11. Diethyl ether, $(C_2H_5)_2O$ (Merch, 99.7%)
12. Eicosane, $C_{20}H_{42}$ (Fluka, ≥97%)
13. N-methyl-N-trimethylsilyltrifluoroacetamide (MSTFA), (Fluka, ≥97%)
14. Methyl oleate standard, $C_{19}H_{36}O_2$ (Aldrich, 99%)

3.3 Modification of bentonite clay

The treated bentonite clay was prepared by treatment of 1 g of raw bentonite clay using 30 ml of 0.5 M aqueous solutions of H_2SO_4 at 120^oC under refluxing for 1 h (3 times). The resulting solid was collected by centrifuged and dried overnight at 100°C. The flowchart for ion-exchange was shown in Scheme 3.1.

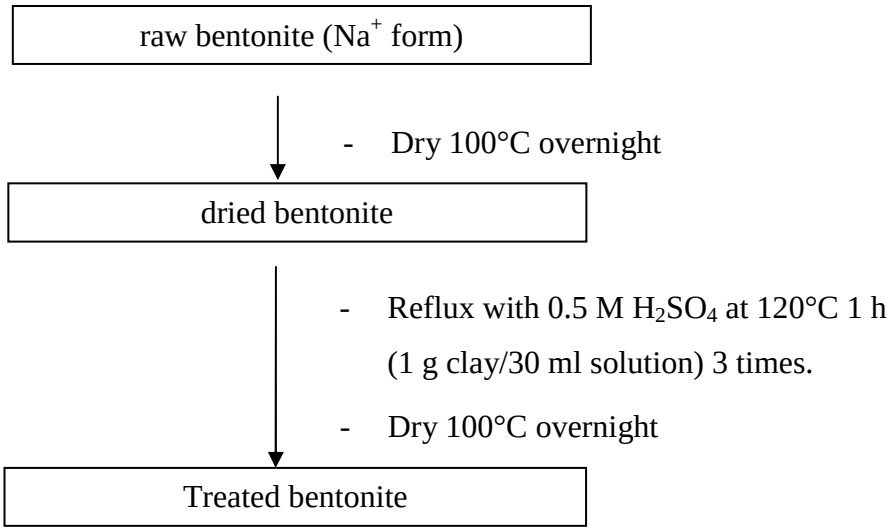

Scheme 3.1 Diagram for modification of bentonite clay.

3.3.1 Acid-base titration

The treated bentonite was acid quantified by using 2 M NaCl solutions as the ion-exchange agent (Scheme 3.2). Approximately 0.05xx g of the catalyst was exchanged with 15 ml of NaCl solution for 30 min under constant agitation at room temperature and titrated with 0.01 M NaOH by using phenolphthalein as indicator [43].

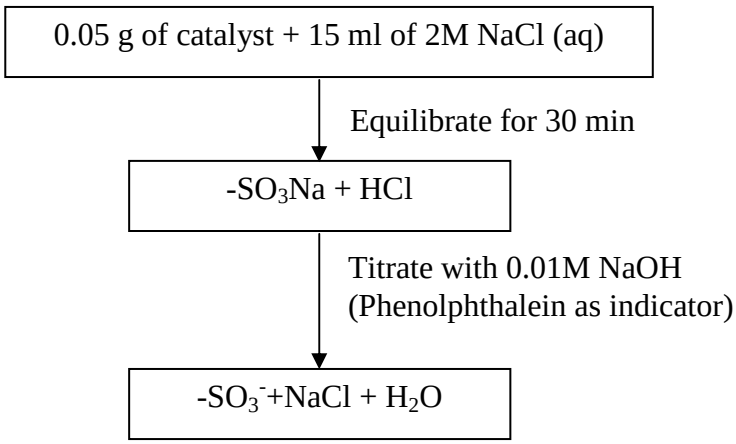

Scheme 3.2 Diagram for acid-base titration.

3.4 Extrusion of bentonite clay

The treated bentonite was shaped in a cylinder form of with a size of 2×2-3 mm (diameter×length) by mixing with a cellulose as a binder and water. Extrusion compositions were bentonite to cellulose as 85:15, 90:10, 95:5 with water 35 wt%, bentonite to SBA-15-Pr-SO_3H as 90:10 with water 35 wt% and pure bentonite with water 35-45 wt%. The extruding catalyst flowchart was shown in (Scheme 3.3).

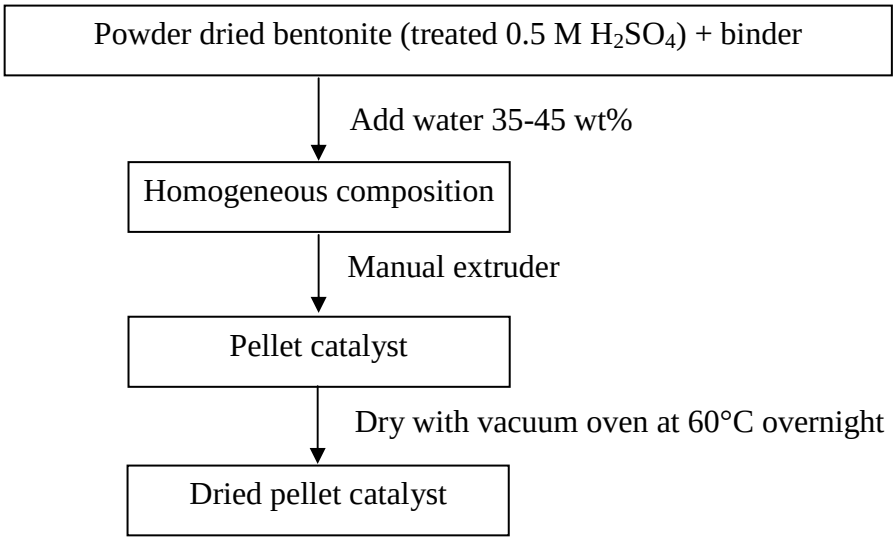

Scheme 3.3 Diagram for extrusion catalyst.

3.4.1 Swelling test [44, 45] (modified from ASTM D 5890-02)

One gram of pellet catalyst with 8 ml of methanol was aged at room temperature for 7 days. The changed volume was observed by using a graduated cylinder.

3.5 Parameters affecting esterification in continuous packed-bed reactor

Esterification of oleic acid 15 wt% in refined palm oil (RPO) and *Jatropha curcas* oil with alcohol (methanol and ethanol) were circulated in five times which separated feed oil and alcohol using a peristaltic pump into a continuous glass packed bed reactor. The product of 1^{st} loop was used as a reactant in the 2^{nd} loop and other

next loop. Reaction temperature was obtained by a heater band that wrapped before a jacket reactor. The experiment setup was showed in Figure 3.2.

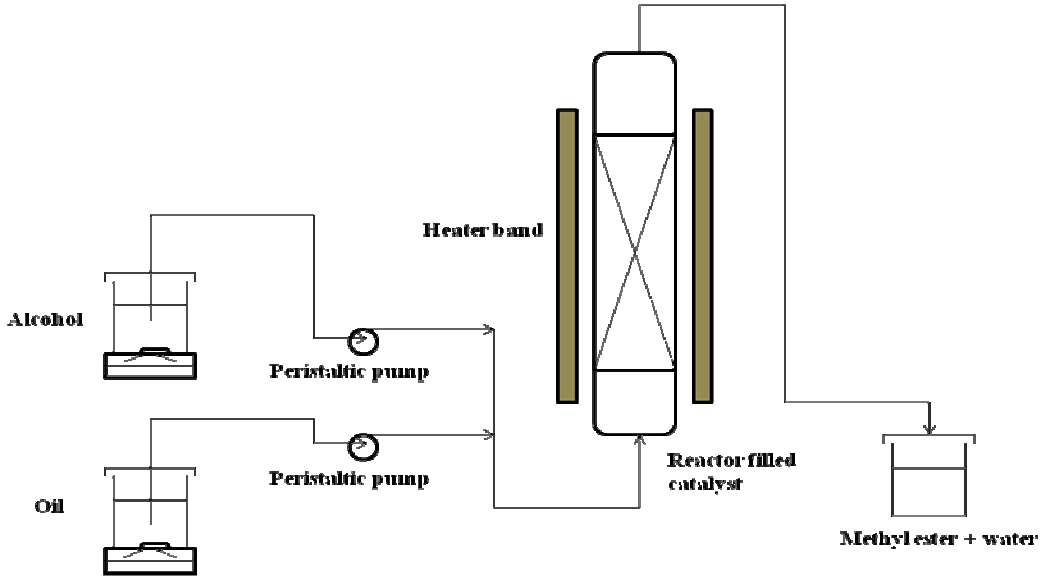

Figure 3.2 Experimental setup for esterification in packed bed reactor under liquid phase system.

3.5.1 Effect of binder in catalysts

The effect of binder mixing in catalyst was studied using the ratio of bentonite to cellulose as 95:5, 90:10 and 85:15 and bentonite to SBA-15-Pr-SO_3H as 90:10 (weight ratio). Esterification of oleic acid 15 wt% in refined palm oil with methanol was performed by fixing oil to methanol mole ratio as 1:23, oil flow rate 0.32 ml/min, catalytic height 25 cm (13.5 g) at 60°C.

3.5.2 Effect of water content in pelletization process

The esterification reaction was carried out in catalytic height 25 cm (13.5 g), oil to methanol mole ratio as 1:23 at 60°C. Water content was varied in range 35, 40 and 45 wt% in the extrusion procedure of pellet-type catalyst.

3.5.3 Effect of oil to alcohol mole ratio

The effect of oil (oleic acid 15 wt% in refined palm oil and *Jatropha curcas* oil) to alcohol (methanol and ethanol) mole ratio was investigated at the value of 1:9, 1:23, 1:54 and 1:70 with catalytic height 25 cm (13.5 g) at reaction temperature 60°C.

Table 3.1 Flow rate of oil and alcohol of each mole ratio.

No.	Mole ratio oil: alcohol	Flow rate of oil (ml/min)	Flow rate of alcohol (ml/min)
1	1:9	0.75	0.32
2	1:23	0.32	0.32
3	1:54	0.32	0.75
4	1:70	0.32	0.97

3.5.4 Effect of the amount of initial free fatty acid

The initial free fatty acid amount was varied in range of 5-15 wt%. The condition was fixed at oil to methanol mole ratio as 1:54, oil flow rate 0.32 ml/min, catalytic height 25 cm (13.5 g) at 60°C.

3.5.5 Effect of reaction temperature

To investigate the effect of temperature in esterification reaction, the reaction was also performed at three reaction temperatures as 50, 60 and 70^{o}C, alcohol (methanol and ethanol) to FFA mole ratio at 54 and catalytic height 25 cm (13.5 g).

3.5.6 Effect of catalytic height

The effect of catalytic height was varied in three parameters at the range of 15-25 cm, all reaction parameters were fixed at methanol to FFA mole ratio as 54:1 and reaction temperature at 60^{o}C.

3.5.7 Two-column reactor

Esterification reaction was also performed as the general procedure above using two-columns reactor, the experiment setup was shown in Figure 3.3.

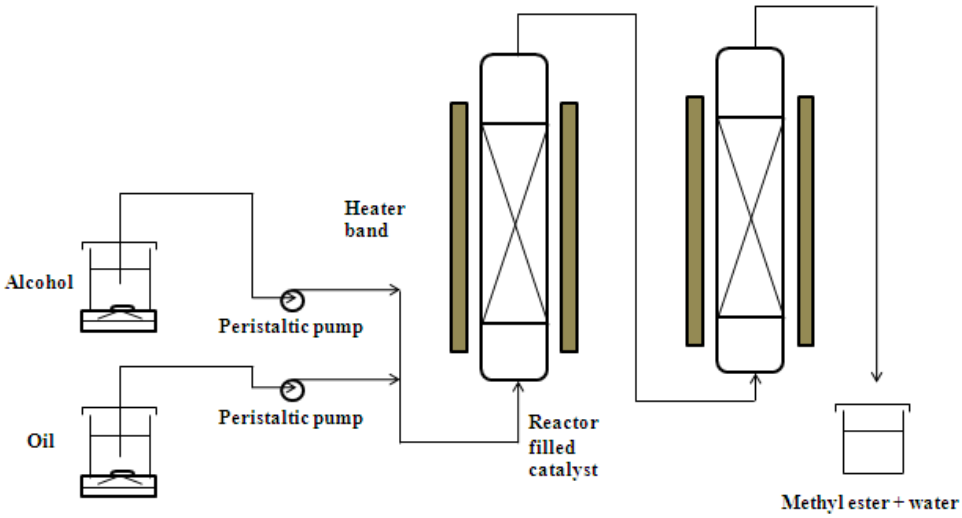

Figure 3.3 Experimental setup for two-column reactor.

3.5.8 Activity of reused catalyst

The used catalyst was washed by feeding methanol into packed-bed reactor until the solution was colorless, after that it was tested catalytic activity again.

CHAPTER IV
RESULTS & DISCUSSIONS

4.2 Physical properties of bentonite clay

The prepared catalyst samples were characterized, elemental analysis by XRF, the crystallinity by X-ray powder diffraction (XRD), the functional groups by attenuated total reflection infrared (ATR-IR) spectroscopy, the morphology by scanning electron microscopy (SEM), the specific surface area by N_2 adsorption-desorption isotherms and thermal stability by Thermogravimetric analysis (TGA). Meanwhile, acid-base titration was performed to quantify the acid strength of the treated bentonite materials.

4.1.1 X-ray fluorescence spectroscopy (XRF)

The chemical composition of natural bentonite (sodium bentonite) and treated bentonite were presented in Table 4.1. The sodium bentonite was mainly composed of SiO_2 and Al_2O_3. The decreasing of cations (Na^+, Ca^{2+}, Mg^{2+}, Al^{3+}, K^+, and Fe^{3+}) was observed that the mentioned cations dissolute from montmorillonite layer after acid treatment. Besides, the SO_3 increasing was obtained from sulfuric solution in acidify process, the contents of Na_2O, CaO and K_2O cations were found in montmorillonite interlayer. The natural bentonite contained higher amount of Na_2O as 3.0% than CaO and K_2O, so this kind indicated as sodium bentonite which was corresponded to data from Volclay Siam Ltd.

Table 4.1 Chemical composition of sodium bentonite and treated bentonite.

Compound	Concentration (%)	
	Sodium bentonite	**Treated bentonite**
SiO_2	68.5	42.3
Al_2O_3	17.0	10.0
Fe_2O_3	4.9	3.1
Na_2O	3.0	0.5
MgO	2.8	1.4
K_2O	1.3	0.8
TiO_2	1.1	0.8
CaO	0.9	0.3
SO_3	0.2	40.7

4.1.2 Powder X-ray diffraction (XRD)

The XRD patterns of sodium bentonite and treated bentonite indicated in Figure 4.1. The sodium bentonite exhibited peaks of montmorillonite with d_{001} and d_{020} value of 1.26 and 0.44 nm, respective [46, 47], and other peaks were non-clay minerals, i.e. quartz and feldspar. The crystallinity of montmorillonite (d_{001} and d_{020}) was decreased from sodium bentonite due to ion-exchange and partial dissolution of cations in structure that confirmed by XRF in Table 4.1. However, the pattern still contained characteristic plane at d_{001} and d_{020} [48].

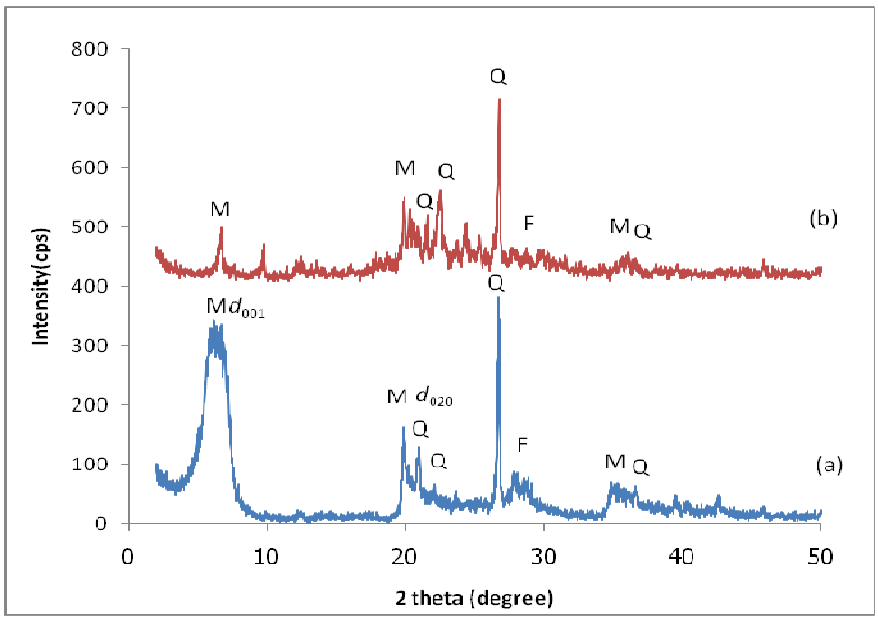

Figure 4.1 XRD patterns of (a) sodium bentonite and (b) treated bentonite (M-montmorillonite, Q-quartz and F-feldspars).

4.1.3 Infrared spectroscopy (IR spectroscopy)

Figure 4.2 and Table 4.2 showed the IR spectra of sodium bentonite and treated bentonite. The absorption band at 3616 cm^{-1} was a stretching vibration of Al-OH groups in bentonite structure. The broad band near 3388 cm^{-1} was due to the hydroxyl stretching vibrations. Moreover, the band at 1626 cm^{-1} was responsible for bending H-O-H vibration in water [49]. Additionally, the band corresponding to Al-Al-OH bending was observed at 914 cm^{-1}. Whereas the very strong absorption band at 972 cm^{-1} was Si-O bending vibration [46]. Acid treatment of clay was known to result in the removal of Al^{3+} and Mg^{2+} ions from the octahedral sheet and migration of other soluble ions into the interlayer that it decreased peak intensity at 3613 cm^{-1} as stretching vibration of Al-OH groups. Meanwhile, the intensity of broad band at 3103 cm^{-1} was increased due to increasing of hydroxyl groups which indicated the amount of acid sites indirectly [49].

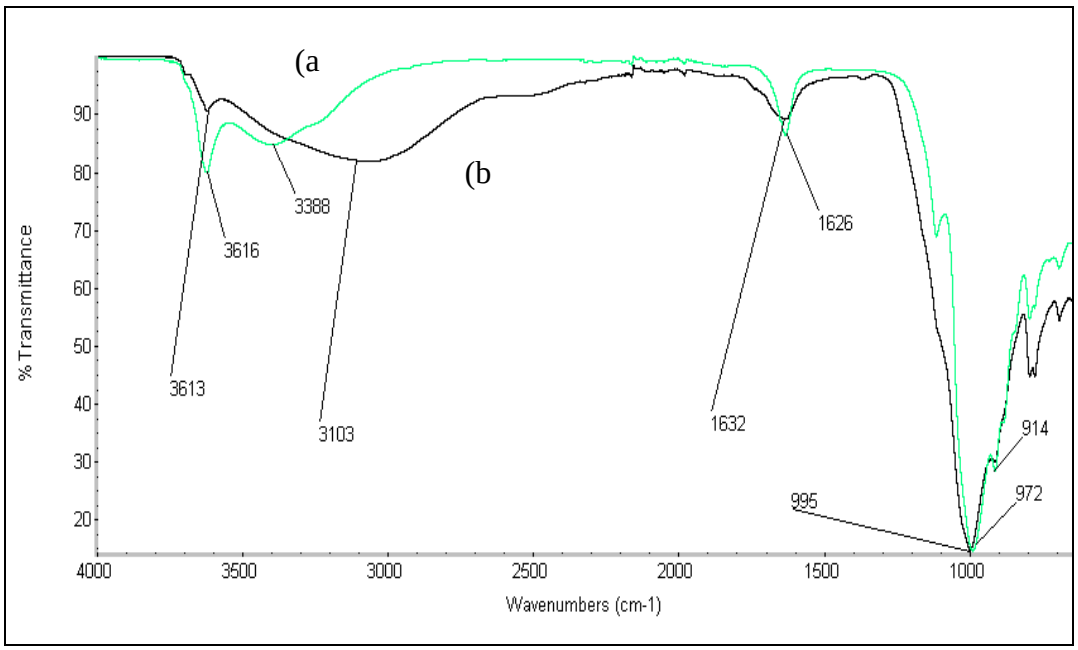

Figure 4.2 ATR-IR spectra of (a) sodium bentonite and (b) treated bentonite.

Table 4.2 Characteristic ATR-IR bands for sodium bentonite and treated bentonite.

Wave number (cm^{-1})		**Band assignment [46, 49]**
Bentonite		
Parent	**Acid**[a]	
3616	3613	Al-OH stretching
3388, 1626	3103 (broad), 1632	H-O-H stretching and bending
972 (strong)	995(strong)	Si-O bending
914	914	Al-Al-OH bending

[a]treated bentonite with 0.5 M H_2SO_4

4.1.4 Scanning Electron Microscopy (SEM)

Figure 4.3 indicated the morphology of sodium bentonite which showed the irregular surface layer. After acid treatment the surface exhibited well-defined sheet as the thin flakes and increased the depth of surface layer (Figure 4.4) which agreed with the increasing surface area in Table 4.3.

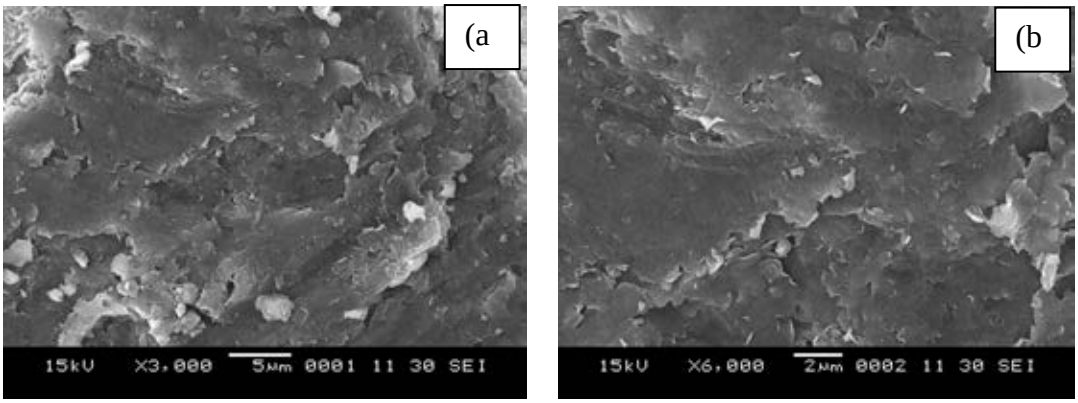

Figure 4.3 SEM images of sodium bentonite at different magnifications: ×3,000 (a), and×6,000 (b).

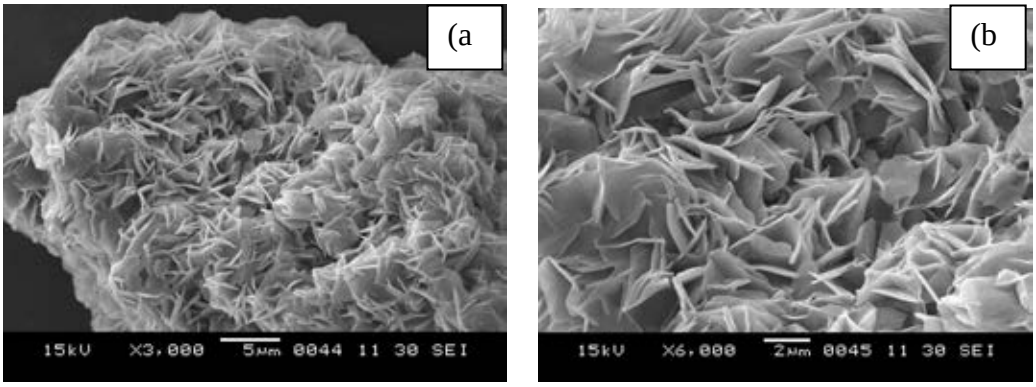

Figure 4.4 SEM images of treated bentonite at different magnifications: ×3,000 (a), and ×6,000 (b).

4.1.5 N_2- adsorption/desorption

The N_2 adsorption-desorption isotherms and pore size distribution of sodium bentonite and treated bentonite showed in Figure 4.5. All results performed type II isotherm of IUPAC classification which was a characteristic pattern of non-porous materials. Some physical properties derived from adsorption isotherms of sodium bentonite and treated bentonite were complied in Table 4.3. The total specific surface area of sodium bentonite, powder treated bentoite and pellet treated bentonite were calculated using Brunauer, Emmett and Teller (BET) equation, which were found at 6, 22 and 15 m^2/g, respectively. Both powder and pellet treated bentonite exhibited higher surface area and pore volume than sodium bentonite due to the partial dissolution of cations such as Na^+, Ca^{2+} and Al^{3+}, Fe^{3+} Mg^{2+} in structure of montmorillonite [47]. This effect could be also observed by SEM images in Figure 4.3 which showed more orderly structure arrangement [47]. The surface area, pore volume and pore diameter of pellet treated bentonite was lower than the powder sample due to inclusion of bentonite molecules inside the pore structure [9].

Table 4.3 Some physical properties of sodium bentonite and treated bentonite.

Sample	Total specific surface area[a] (m^2g^{-1})	Total pore volume[b] (cm^3g^{-1})	Average pore diameter (nm)
Sodium bentonite	6	0.03	2.4
Powder treated bentonite (0.5 M H_2SO_4)	22	0.12	21.3
Pellet treated bentonite (0.5 M H_2SO_4)	15	0.06	3.3

[a]Calculated using the BET plot method
[b]Calculated using the BJH method,

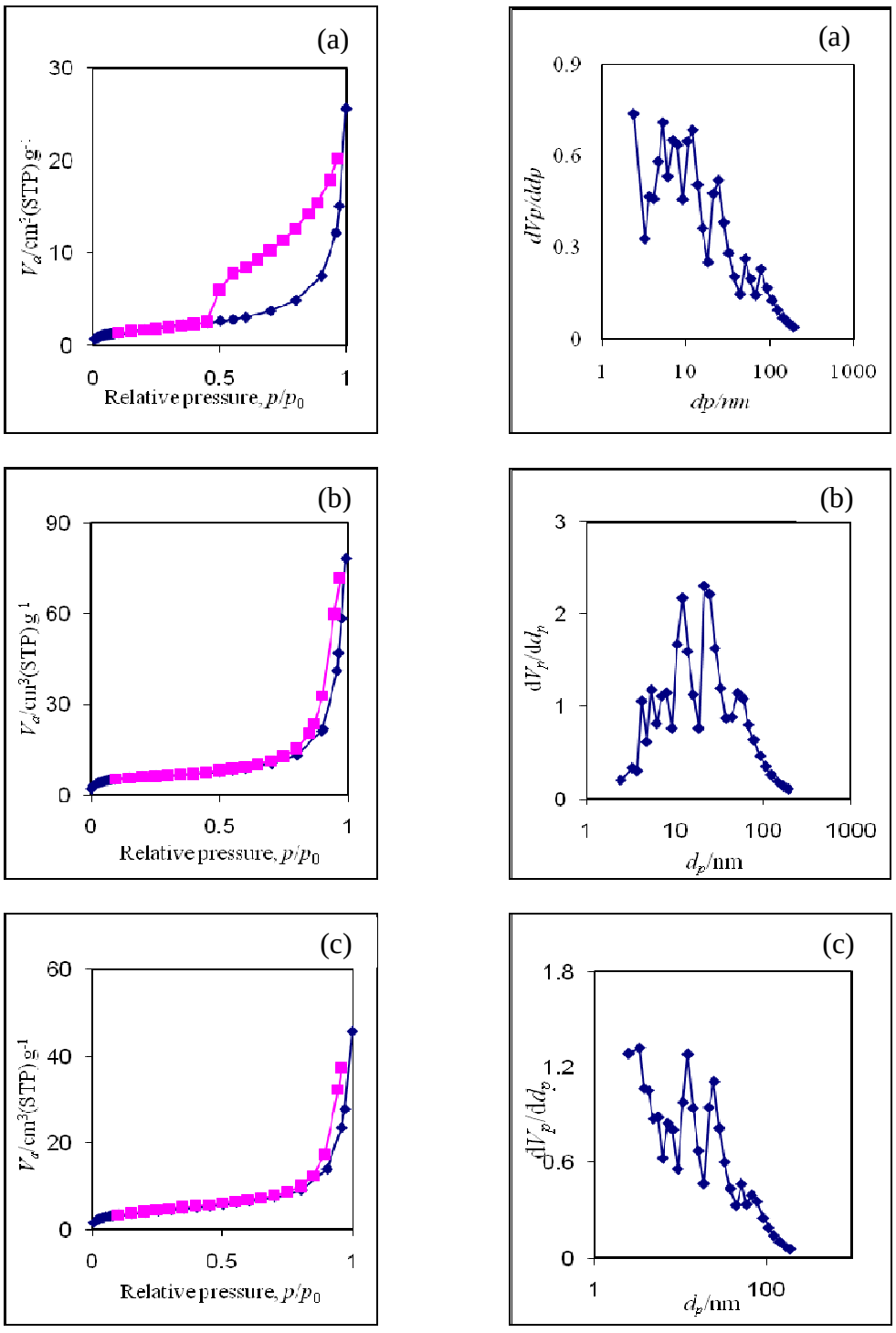

Figure 4.5 N_2 adsorption-desorption isotherms and BJH-pore size distribution of (a) Sodium bentonite (b) Powder treated bentonite and (c) Pellet treated bentonite.

4.1.6 Thermogravimetric analysis (TGA)

Figure 4.6 showed an example of TGA and DTG curves of treated bentonite. The modification of bentonite indicated two step weight losses in TG patterns as 24.55% and 19.26% at temperature in the range of 40-200°C and 400-800°C, respectively. Whereas the differential thermal analysis (DTA) curve exhibited the losses of two endothermic peaks at 118.3°C and 761.2°C which might be caused by losing physisorbed water and chemisorbed of sulfuric acid [50].

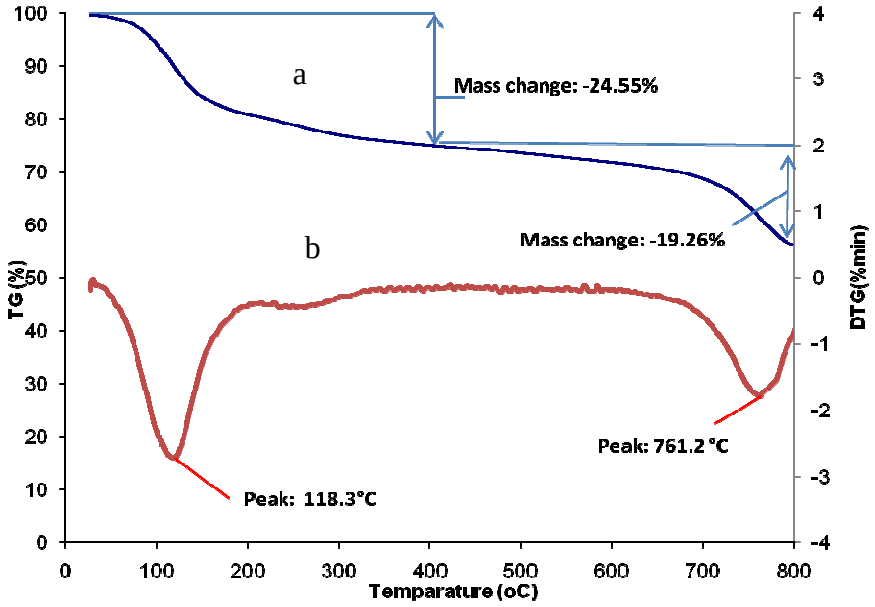

Figure 4.6 TGA (a) and DTG (b) curves of treated bentonite.

4.1.7 Acid-base titration

The number of sulfonic acid sites in the treated bentonites was quantitatively measured by acid-base titration using sodium chloride as ion-exchange agent which the result was shown in Table 4.4. The acid value of treated bentonite performed higher than the sodium bentonite that could be observed by higher absorption of H-O-H vibration at 3103 cm^{-1} [49].

Table 4.4 Acid value of sodium bentonite and treated bentonite.

Catalyst	H^+ content[a] (mmol/g)
Sodium bentonite	0.2
Treated bentonite (0.5 M H_2SO_4)	2.0

[a]Acid capacity defined as millimole of acid centers per gram of catalyst

4.2 Swelling test

Table 4.5 showed swelling test of treated bentonite pellet, which mixed with 35 wt% water and cellulose in ratio of bentonite to binder as 95:5, 90:10 and 85:15 or mixed with SBA-15-Pr-SO_3H in ratio 90:10, respectively. After swelling for a week, all were observed no catalytic swollen which pelletized by extrusion. On the other hand, methanol color was changed from colorless to orange because of acid leaching out which was described by changing of pH value from 5.14 to 0.9.

Table 4.5 Swelling of all catalysts.

Catalyst	Volume (cm^3/g)			Swollen (%)
	Start volume of catalyst	After add methanol	After 1 week	
a	1.2	1.2	1.2	0
b	1.3	1.3	1.3	0
c	1.3	1.3	1.3	0
d	1.4	1.4	1.4	0
e	1.3	1.3	1.3	0

a=treated bentonite
b=treated bentonite+cellulose (95:5)
c=treated bentonite+cellulose (90:10)
d=treated bentonite+cellulose (85:15)
e=treated bentonite+SBA-15-Pr-SO_3H (90:10)

4.3 Catalytic activity of treated bentonite in esterification reaction of free fatty acid

4.3.1 Effect of binder in catalysts

From estimation, cellulose might facilitate in pelletization process, mixing cellulose as a binder in extrusion process was studied. Treated bentonite was mixed with cellulose in the weight ratio of 95:5, 90:10 and 85:15 with 35 wt% water. Moreover, treated bentonite was also mixed with SBA-15-Pr-SO_3H in the ratio 90:10 with 35 wt% of water.

Table 4.6 indicated FFA conversion of esterification between oleic acid in refined palm oil (RPO) with methanol under mole ratio of oil to methanol as 1:23 with 25 cm (13.5 g) catalytic height in a continuous packed bed reactor at reaction temperature 60^{o}C. The weight ratio of cellulose to bentonite was varied from 5 to 15 wt%. The increasing cellulose content could decline FFA conversion owing to the decreasing amount of acid site in catalyst. However, the high FFA conversions were obtained by using treated bentonite, the mixture of treated bentonite with cellulose in ratio 95:5 and mixture of treated bentonite with SBA-15-Pr-SO_3H in 90:10 as catalyst which provided the minimum FFA as 1.5, 1.4 and 1.7 at the 5th loop, respectively. As a result, adding binder into effective material could not promote significantly difference on esterification. Thus, treated bentonite was selected as catalyst in subsequent experiments due to low cost and no significant of hardness. Beside, treated bentonite was easier preparation than SBA-15-Pr-SO_3H process.

Table 4.6 The catalytic activities of mixture binder with catalysts in esterification reaction of oleic acid with methanol.

Sample	FFA, as oleic acid (%conversion)				
	Mixture of catalysts				
	Treated bentonite	**Treated+ cellulose (95:5)**	**Treated+ cellulose (90:10)**	**Treated+ cellulose (85:15)**	**Treated+ SBA-15-Pr-SO_3H (90:10)**
Refined palm oil+15 wt% oleic acid	14.0	14.0	14.3	15.1	14.0
1st loop	6.1(56.4)	5.7(59.3)	5.8(59.4)	7.2(52.3)	5.7(59.3)
2nd loop	3.8(72.9)	4.0(71.4)	5.1(64.3)	5.5(63.6)	3.8(72.9)
3rd loop	2.6(81.4)	2.4(82.9)	3.0(79.0)	3.9(74.2)	2.5(82.1)
4th loop	2.1(85.0)	1.9(86.4)	2.8(80.4)	3.7(75.5)	1.9(86.4)
5th loop	1.5(89.3)	1.4(90.0)	2.2(84.6)	3.2(78.8)	1.7(87.9)

Reaction condition: mole ratio of oil to methanol as 1:23, catalytic height 25 cm (13.5 g) and temperature 60°C, LHSV1.5 hr^{-1}.

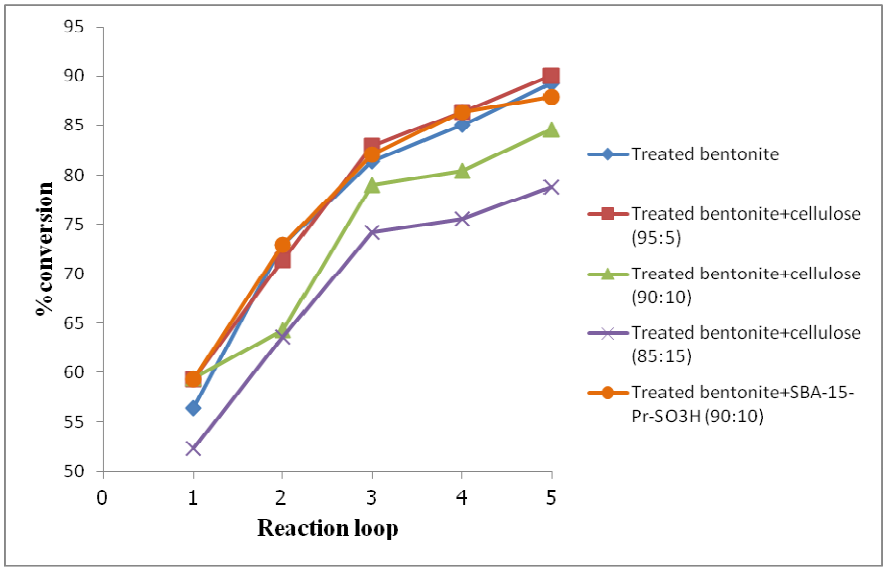

Figure 4.7 Conversion of mixture binder with catalyst in esterification reaction of oleic acid with methanol.

4.3.2 Effect of water content in pelletization process

In the process of catalyst extrusion, water was used to make it easier in the extrusion process. Thus the water content was varied in range of 35-45 wt%. Then the extruded catalysts were dried in vacuum oven at 60°C for 24 hours. The resulted catalyst pellet appeared white color and sized as 2x2-3 mm.

Esterification of oleic acid in refined palm oil (RPO) with methanol was shown in Table 4.7 and Figure 4.8. The reaction was performed by fixing mole ratio of oil to methanol as 1:23 in 25 cm (13.5 g) catalytic height in a continuous packed bed reactor at reaction temperature 60^{o}C. The result showed no significant difference in FFA conversion that water content in extrusion process was not impact on the catalytic activity which could observe by FFA conversion. The observation could be explained by the complete evaporation of water in drying process. Thus, the water content 35 wt% was selected for mixing in extrusion step in this research.

Table 4.7 The effect of water content in pelletization process for esterification reaction of oleic acid with methanol over treated bentonite.

Sample	FFA, as oleic acid (%conversion)		
	Water content		
	H_2O 35 wt%	H_2O 40 wt%	H_2O 45 wt%
Refined palm oil+15 wt% oleic acid	14.0	14.0	14.1
1st loop	6.1(56.4)	6.1(56.4)	5.8(58.9)
2nd loop	3.8(72.9)	3.4(75.7)	3.7(73.8)
3rd loop	2.6(81.4)	2.4(82.9)	2.0(85.8)
4th loop	2.1(85.0)	1.6(88.6)	1.8(87.2)
5th loop	1.5(89.3)	1.3(90.7)	1.4(90.1)

Reaction condition: mole ratio of oil to methanol as 1:23, catalytic height 25 cm (13.5 g) and temperature 60^{o}C, LHSV 1.5 hr^{-1}.

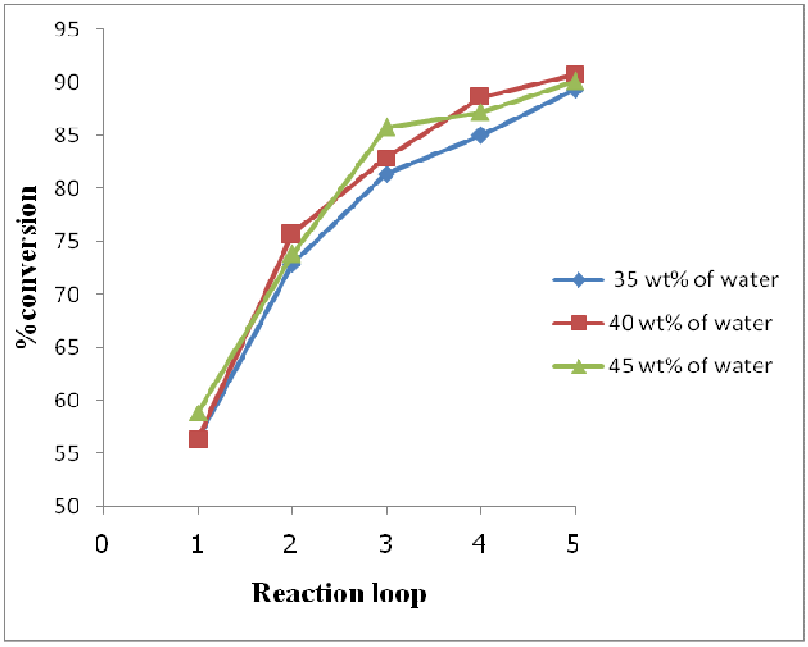

Figure 4.8 Conversion of water content in treated bentonite for extrusion process.

4.3.3 Effect of oil to alcohol mole ratio

4.3.3.1 Methanol

Effect of oil to methanol mole ratio in esterification of oleic acid with methanol was indicated in Table 4.8 and Figure 4.9. The reaction condition was fixed catalyst height and reaction temperature as 25 cm and 60^{o}C. When the mole ratio of oil to methanol was enhanced from 1:9 to 1:70, FFA conversion gave higher from 42.6 to 69.9% in the 1st loop and 88.2 to 92.6% in the 5th loop. This effect might be explained by high amount of methanol which could increase solubility and contact between oil and methanol molecules in a continuous packed bed reactor [14, 51]. The esterification is an equilibrium reaction which a high amount of methanol is used to drive the reaction to the right. Nevertheless, the high amount of methanol also gave water as by-product which reversible reaction could occur to reduce methyl ester product [51]. However, the result was incompatible with result of LHSV. The high value of LHSV exhibited high feed rate of reactant that reduced contact time between starting materials with catalytic phase in a continuous packed bed reactor. Although the mole ratio of oil to methanol as 1:70 performed highest LHSV as 2.90 hr^{-1}but this ratio gave highest FFA conversion. Then, the effect of solubility between starting

materials was more important than the result of contact time. However, the highest FFA conversion was obtained as 92.6% in the 5th loop with 1:54 and 1:70 of oil to methanol mole ratio. Moreover, these two mole ratios were no significantly difference of FFA conversion since the 2rd to 5th loops thus mole ratio of oil to methanol as 1:54 was selected for subsequent experiments.

Table 4.8 The effect of oil to methanol mole ratio for esterification between oleic acid with methanol over treated bentonite.

Sample	FFA, as oleic acid (%conversion)			
	Mole ratio of oil to methanol			
	1:9	**1:23**	**1:54**	**1:70**
Refined palm oil+15 wt% oleic acid	13.6	14.0	13.6	13.6
1st loop	7.8(42.6)	6.1(56.4)	4.8(64.7)	4.1(69.9)
2nd loop	4.2(69.1)	3.8(72.9)	2.5(81.6)	2.0(85.3)
3rd loop	3.0(77.9)	2.6(81.4)	1.6(88.2)	1.5(89.0)
4th loop	2.3(83.1)	2.1(85.0)	1.2(91.2)	1.3(90.4)
5th loop	1.6(88.2)	1.5(89.3)	1.0(92.6)	1.0(92.6)

Reaction condition: catalytic height 25 cm (13.5 g) and temperature 60^{o}C, LHSV as 2.4, 1.5, 2.4 and 2.9 hr^{-1}for mole ratio 1:9, 1:23, 1:54 and 1:70, respectively.

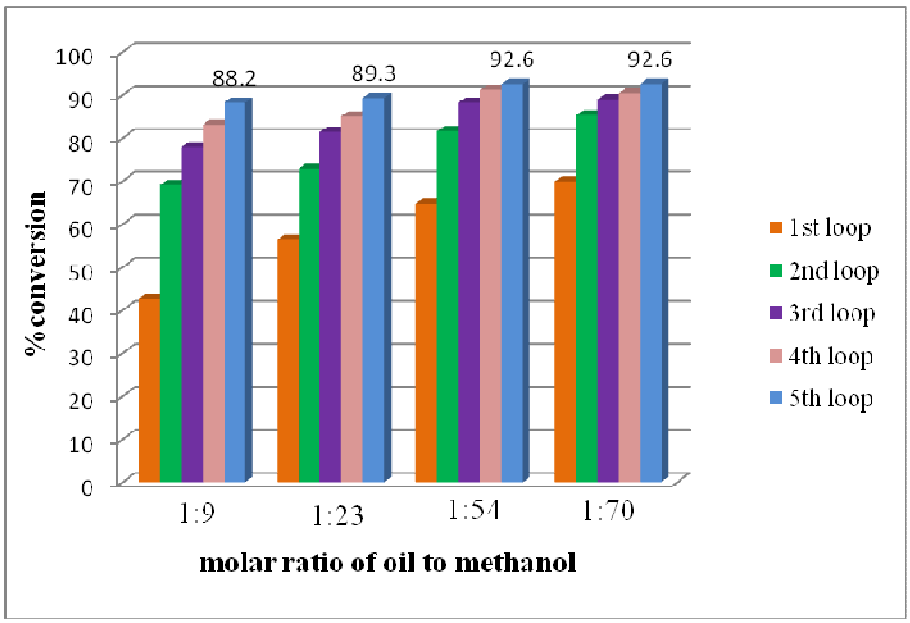

Figure 4.9 Conversion of oleic acid in various oil to methanol mole ratio over treated bentonite.

4.3.3.2 Ethanol

Table 4.9 and Figure 4.10 exhibited effect of oil to ethanol mole ratio of oleic acid in RPO esterification with ethanol. The reactions were fixed catalytic height as 25 cm at 60^{o}C. The mole ratio of oil to ethanol was varied from 1:23 to 1:70 which the result revealed higher FFA conversion from 67.9 to 82.6% in the 1st loop and 88.8 to 96.4% in the 5th loop when higher oil to ethanol ratio. So, an increasing of FFA conversion could be explained in the similar way was as methanol in term of the solubility between ethanol and oil which resulted in Table 4.8. However, the highest FFA conversion was obtained at mole ratio 1:70 which increased from 82.6 to 96.4% in the 1st to 5th loops. Nevertheless, this mole ratio exhibited no significant difference to 1:54 mole ratio since the 3rd loop. Thus, the mole ratio as 1:54 was suitable for subsequent system. Additionally, the result shows that the esterification of ethanol provided higher FFA conversion than the methanol due to increasing FFA solubility in longer hydrocarbon chain of alcohol in reactor.

Table 4.9 The effect of oil to ethanol mole ratio for esterification between oleic acid with ethanol over treated bentonite.

Sample	FFA, as oleic acid (%conversion)		
	Mole ratio of oil to ethanol		
	1:23	**1:54**	**1:70**
Refined palm oil +15 wt% oleic acid	13.4	13.7	13.8
1st loop	4.3(67.9)	4.1(70.1)	2.4(82.6)
2nd loop	3.2(76.1)	2.3(83.2)	1.3(90.6)
3rd loop	1.8(86.6)	1.4(89.8)	1.2(91.3)
4th loop	1.7(87.3)	0.9(93.4)	0.7(94.9)
5th loop	1.5(88.8)	0.7(94.9)	0.5(96.4)

Reaction condition: catalytic height 25 cm (13.5 g) and temperature 60°C, LHSV as 1.5, 2.4 and 2.9 hr^{-1} for mole ratio 1:23, 1:54 and 1:70, respectively.

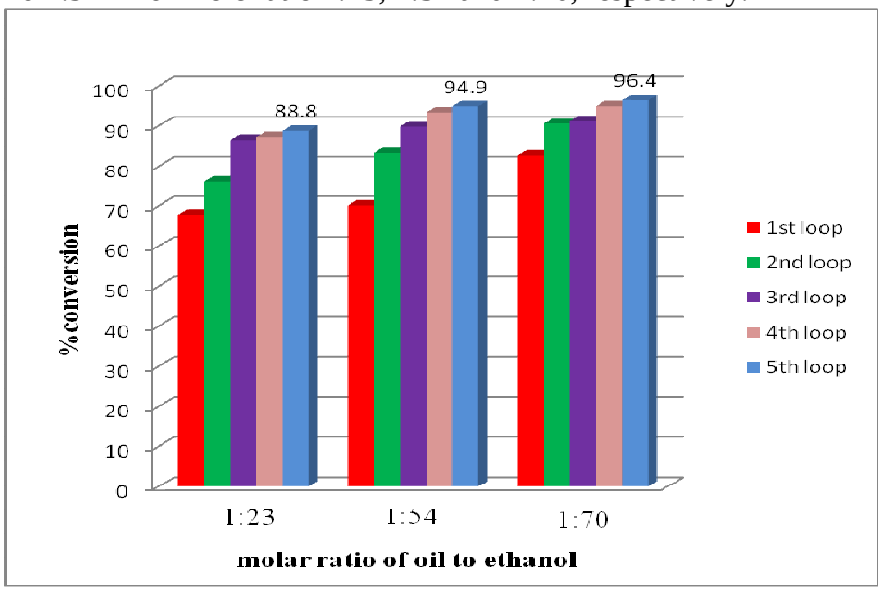

Figure 4.10 Conversion of oleic acid in various oil to ethanol mole ratio over treated bentonite.

4.3.4 Effect of the amount of initial free fatty acid

In this case the percentage of initial free fatty acid was varied in range of 5-15 wt% in esterification of oleic acid with methanol over treated bentonite. The reaction condition performed at 60^{o}C in 25 cm catalytic height using mole ratio of oil to methanol as 1:54. The results were shown in Table 4.10 and Figure 4.11. When the amount of initial FFA was increased, it performed higher reaction rate at the 1st loop (high conversion). Nevertheless, the 3rd to 5th loop gave percentage of FFA residue close to each reaction due to decreasing catalyst effective [52]. Additionally, the remained FFA was obtained only 1.0% in 5th loop for all three trials. While, biodiesel production was recently produced from high FFA containing in oil due to low cost of raw material. The treated bentonite catalyst could use with low quality oil for biodiesel production. Thus, the FFA 15 wt% was selected to add in refined palm oil for esterification in the next experiments.

Table 4.10 The effect of the amount of initial free fatty acid for esterification between oleic acid with methanol over treated bentonite.

Sample	**FFA, as oleic acid (%conversion)**		
	Oleic acid in refined palm oil		
	Oleic acid 5 wt%	**Oleic acid 10 wt%**	**Oleic acid 15 wt%**
Refined palm oil + oleic acid	5.2	9.8	13.6
1st loop	2.2(57.7)	4.1(58.2)	4.8(64.7)
2nd loop	1.6(69.2)	1.9(80.6)	2.5(81.6)
3rd loop	1.5(71.2)	1.5(84.7)	1.6(88.2)
4th loop	1.1(78.8)	1.3(86.7)	1.2(91.2)
5th loop	1.0(80.8)	1.0(89.8)	1.0(92.6)

Reaction condition: mole ratio of oil to methanol as 1:54, catalytic height 25 cm (13.5 g) and temperature 60^{o}C, LHSV 2.4 hr^{-1}.

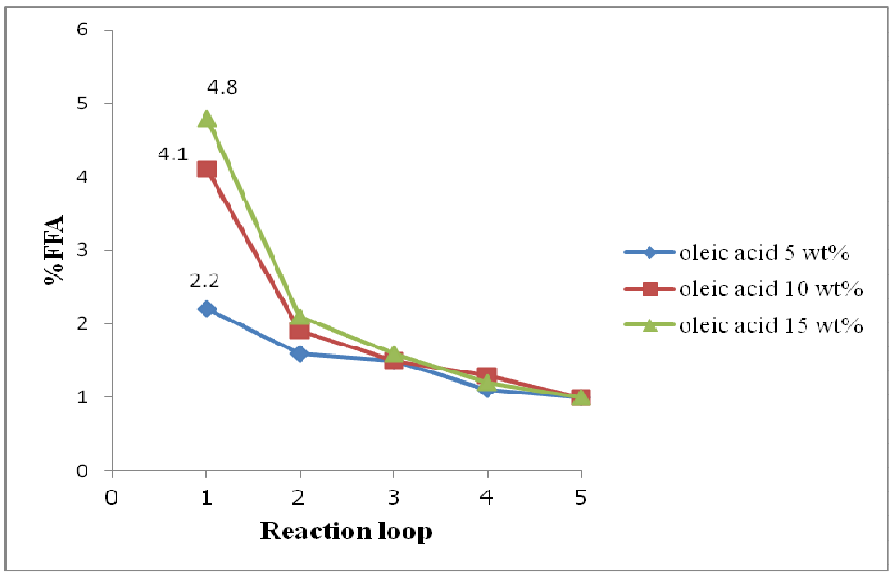

Figure 4.11 The FFA percentage of amount of initial free fatty acid.

4.3.5 Effect of reaction temperature

4.3.5.1 Methanol

The reaction temperature was varied in range of 50-70°C using treated bentonite as catalyst. The condition was fixed mole ratio of oil to methanol as 1:54 and catalytic height 25 cm (13.5 g). The experimental result was shown in Table 4.11 and Figure 4.12. The reaction temperature at 60^{o}C provided higher FFA conversion than 50^{o}C due to higher reaction rate. When the reaction temperature was elevated above the methanol boiling point (65^{o}C), it exhibited the decreasing FFA conversion. Because the methanol bubbles ran out rapidly from reactor, resulting in a reduction of the mole ratio of methanol to oil and a decreasing of the contact between starting materials with catalyst phase inside a packed bed reactor. The highest FFA conversion was obtained as 92.6% in the 5th loop at temperature 60°C. Therefore, the reaction temperature at 60°C was selected for further esterification of methanol to investigate in other reaction parameter effects.

Table 4.11 The effect of reaction temperature for esterification between oleic acid with methanol over treated bentonite.

Sample	FFA, as oleic acid (%conversion)		
	Reaction temperature (^{o}C)		
	50^{o}C	**60^{o}C**	**70^{o}C**
Refined palm oil +15 wt % oleic acid	13.9	13.6	13.9
1st loop	5.4(61.2)	4.8(64.7)	5.5(60.4)
2nd loop	3.6(74.1)	2.5(81.6)	4.0(71.2)
3rd loop	3.3(76.3)	1.6(88.2)	3.8(72.7)
4th loop	2.7(80.6)	1.2(91.2)	2.9(79.1)
5th loop	1.9(86.3)	1.0(92.6)	2.1(84.9)

Reaction condition: mole ratio of oil to methanol as 1:54, catalytic height 25 cm (13.5 g), LHSV 2.4 hr^{-1}.

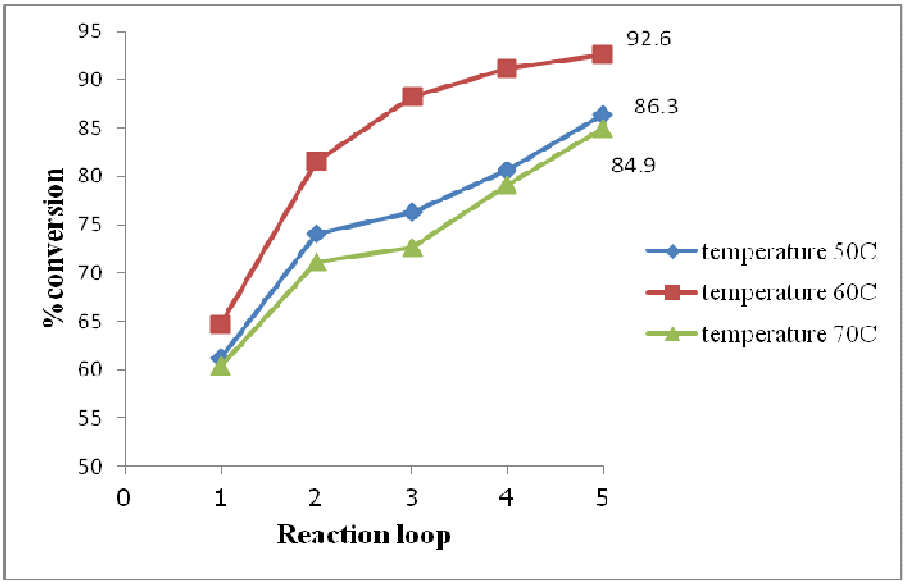

Figure 4.12 Conversion of reaction temperature as 50, 60 and 70 °C for esterification between oleic acid with methanol.

4.3.5.2 Ethanol

Effect of reaction temperature of esterification of oil with ethanol was also varied in range of 50-70°C using treated bentonite as catalyst similar to previous experiment. The reaction condition was fixed mole ratio of oil to ethanol as 1:54, catalytic height 25 cm (13.5 g). The result showed in Table 4.12 and Figure 4.13. The highest FFA conversion was obtained as 94.9% with remaining FFA as 0.7% from 13.7% of initial FFA at 60°C. The reaction temperature at 70°C was found partially ethanol loss which this effect reduced mole ratio of oil to ethanol. Meanwhile, temperature at 50°C was obtained lowest FFA conversion due to low reaction rate in esterification. Thus, temperature at 60°C was selected for esterification of ethanol in the next effects which was consistent with the results of methanol in section 4.3.5.1. Moreover, the comparison in each reaction temperature between methanol and ethanol was found that the esterification of ethanol provided higher FFA conversion than the methanol due to high hydrophobicity of ethanol to increase solubility of FFA starting materials.

Table 4.12 The effect of reaction temperature of esterification between oleic acid with ethanol over treated bentonite.

Sample	FFA, as oleic acid (%conversion)		
	Reaction temperature (^{o}C)		
	50^{o}C	**60^{o}C**	**70^{o}C**
Refined palm oil +15 wt % oleic acid	14.6	13.7	13.9
1st loop	4.9(66.4)	4.1(70.1)	4.9(64.7)
2nd loop	3.5(76.0)	2.3(83.2)	3.2(77.0)
3rd loop	3.3(77.4)	1.4(89.8)	2.6(81.3)
4th loop	2.6(82.2)	0.9(93.4)	2.1(84.9)
5th loop	1.4(90.4)	0.7(94.9)	1.2(91.4)

Reaction condition: mole ratio of oil to ethanol as 1:54, catalytic height 25 cm (13.5 g), LHSV 2.4 hr^{-1}.

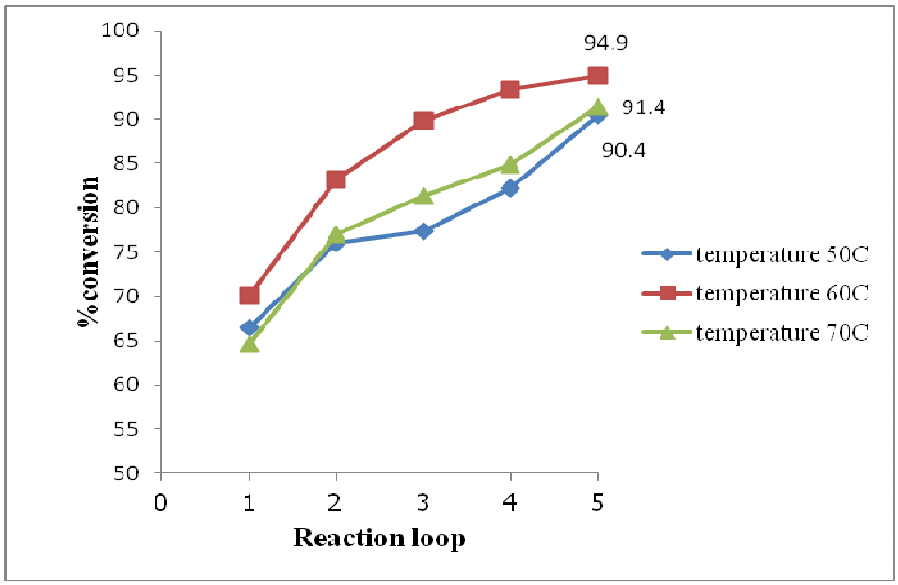

Figure 4.13 Conversion of reaction temperature as 50, 60 and 70 °C for esterification between oleic acid with ethanol.

4.3.6 Effect of catalytic height

Table 4.13 and Figure 4.14 showed the result of varying catalytic height as 15, 20 and 25 cm (8.75, 11.3 and 13.5 g) for esterification of oleic acid in RPO with methanol over treated bentonite. The reaction condition performed with mole ratio of oil to methanol as 1:54 at 60^{o}C. The result obtained higher FFA conversion when increased catalytic height because the contact time between starting materials and catalyst phase was extended [53]. As a result, only the catalytic height at 25 cm obtained FFA conversion over 90% since the 4th loop. Thus, in this work the catalytic height 25 cm was selected for esterification in the experiments. Furthermore, increasing of catalytic height was extended by make two-column parallel reactor in next studying effect.

Table 4.13 The effect of catalytic height of esterification between oleic acid with methanol over treated bentonite.

Sample	FFA, as oleic acid (%conversion)		
	Height of catalyst in packed bed reactor		
	15 cm	**20 cm**	**25 cm**
Refined palm oil +15 wt % oleic acid	14.6	14.6	13.6
1st loop	5.9(59.6)	5.7(61.0)	4.8(64.7)
2nd loop	5.6(61.6)	3.8(74.0)	2.5(81.6)
3rd loop	4.1(71.9)	3.4(76.7)	1.6(88.2)
4th loop	3.3(77.4)	3.0(79.5)	1.2(91.2)
5th loop	3.2(78.1)	2.7(81.5)	1.0(92.6)

Reaction condition: mole ratio of oil to methanol as 1:54, reaction temperature 60^{o}C, LHSV 2.4 hr^{-1}.

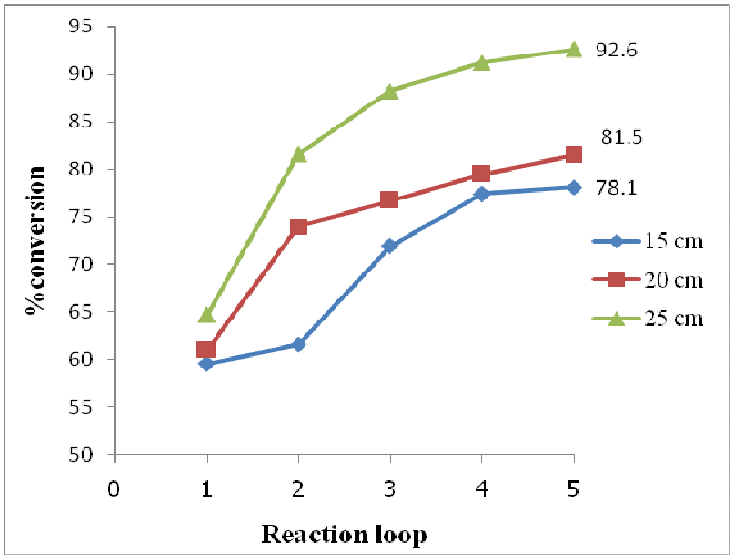

Figure 4.14 Conversion of catalytic height in esterification between oleic acid with methanol over treated bentonite as catalyst.

4.3.7 Two-column reactor

Table 4.14 and Figure 4.15 indicated esterification between oleic acid with methanol and ethanol which performed in two-column reactor. The experiment was carried out using mole ratio of oil to alcohol as 1:54 with catalytic height 25 cm for each reactor at 60^{o}C. When comparison with one-column reactor (Table 4.8 and 4.9), the result obtained a higher FFA conversion than one-column reactor due to higher contact time between starting materials with catalytic phase inside a packed bed reactor. However, esterification of oleic acid in refined palm oil (RPO) with ethanol obtained higher FFA conversion than methanol due to increasing FFA solubility in longer hydrocarbon chain of alcohol. The result of two-column reactor was consistent with one-column reactor. Besides, the percentage of FFA in oil for two-column reactor was reduced from about 14.0% to 0.3% (97.9% conversion) and 0.2% (98.6% conversion) in the 5th loop for methanol and ethanol, respectively. Two-column reactors could reduce the FFA content lower than 1 wt% since the 3rd loop. Moreover, two-column reactors could be carried out in tranesterification process faster than one-column reactor for biodiesel production.

Table 4.14 Comparison of esterification between oleic acid with methanol and ethanol over treated bentonite for one and two-column reactors.

Sample	FFA, as oleic acid (%conversion)			
	Methanol		Ethanol	
	One-column	Two-column	One-column	Two-column
Refined palm oil +15 wt % oleic acid	13.6	14.0	13.7	14.2
1st loop	4.8(64.7)	3.1(77.9)	4.1(70.1)	2.5(82.4)
2nd loop	2.5(81.6)	1.9(86.5)	2.3(83.2)	1.7(88.0)
3rd loop	1.6(88.2)	0.8(94.3)	1.4(89.8)	0.6(95.8)
4th loop	1.2(91.2)	0.7(95.0)	0.9(93.4)	0.3(97.9)
5th loop	1.0(92.6)	0.3(97.9)	0.7(94.9)	0.2(98.6)

Reaction condition: mole ratio of oil to alcohol as 1:54, catalytic height 25 cm, reaction temperature 60°C, LHSV 2.4 hr^{-1}.

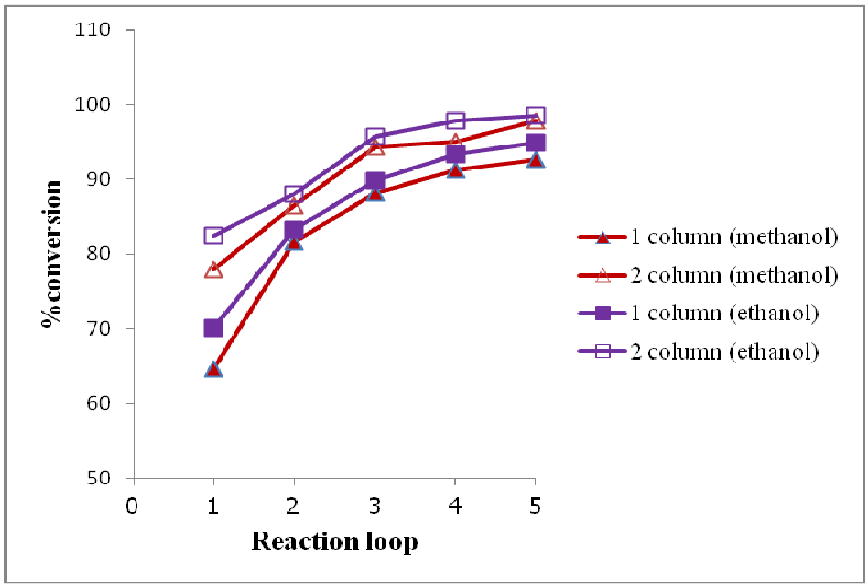

Figure 4.15 Comparison of FFA conversion between one and two-column reactors in esterification between oleic acid with methanol and ethanol.

4.3.8 Type of oil

4.3.8.1 Reaction between *Jatropha curcas* oil with methanol

From previous experiments, the optimal condition which gave highest FFA conversion was obtained over mole ratio of oil to methanol as 1:54, with catalytic height 25 cm (13.5 g) at reaction temperature 60^{o}C for esterification of oleic acid in RPO with methanol. So, this condition of oleic acid with methanol was used to study the reaction of *Jatropha curcas* oil with methanol. The result was indicated in Table 4.15. Comparing the results between the reaction of oleic acid in RPO and *Jatropha curcas* oil with methanol, the reaction of oleic acid in RPO with methanol gave higher FFA conversion because starting oil contained only oleic acid. While the compositions of *Jatropha curcas* oil composed of various free fatty acids both unsaturated and saturated free fatty acids such as the oleic acid, linoleic acid, palmitic acid and the stearic acid which could be different in the optimum condition for esterification. However, unsaturated fatty acids could be easier esterified than saturated fatty acids due to containing double bond in chain. Thus, the highest FFA conversion of *Jatropha curcas* oil with methanol was only 78.3% (FFA as 3.4%) in the 5th loop of reaction.

Table 4.15 Comparison of FFA conversion between oleic acid in refined palm oil and *Jatropha curcas* oil with methanol over treated bentonite.

Sample	FFA, as oleic acid (%conversion)	
	Types of oil	
	Oleic acid in refined palm oil	***Jatropha curcas* oil**
Starting of %FFA	13.6	15.7
1st loop	4.8(64.7)	5.4(65.6)
2nd loop	2.5(81.6)	4.8(69.4)
3rd loop	1.6(88.2)	4.0(74.5)
4th loop	1.2(91.2)	3.6(77.0)
5th loop	1.0(92.6)	3.4(78.3)

Reaction condition: mole ratio of oil to methanol as 1:54, catalytic height 25 cm, reaction temperature 60^{o}C, LHSV 2.4 hr^{-1}.

4.3.8.2 Reaction between *Jatropha curcas* oil with ethanol

Table 4.16 showed result of esterification between *Jatropha curcas* oil and oleic acid in RPO with ethanol which using ratio of oil to ethanol as 1:54 and catalyst height 25 cm (13.5 g) at 60^{o}C. The esterification of oleic acid in RPO with ethanol gave higher FFA conversion than reaction of *Jatropha curcas* oil at the same reaction condition because containing only oleic acid could be easier in esterification. This result was consistent to the effects of alcohol type that showed in section 4.3.3. The percentage of FFA in oil was reduced from 14.9% to 2.0% (86.6% conversion) in the 5th loop for *Jatropha curcas* oil with ethanol.

Table 4.16 Comparison of FFA conversion between oleic acid in refined palm oil and *Jatropha curcas* oil with ethanol over treated bentonite.

Sample	FFA, as oleic acid (%conversion)	
	Type of oil	
	Oleic acid in refined palm oil	***Jatropha curcas* oil**
Starting of %FFA	13.7	14.9
1st loop	4.1(70.1)	4.6(69.1)
2nd loop	2.3(83.2)	4.2(71.8)
3rd loop	1.4(89.8)	3.7(75.2)
4th loop	0.9(93.4)	2.9(80.5)
5th loop	0.7(94.9)	2.0(86.6)

Reaction condition: mole ratio of oil to ethanol as 1:54, catalytic height 25 cm, reaction temperature 60^{o}C, LHSV 2.4 hr^{-1}.

Figure 4.16 indicated relationship between reaction loop and %conversion of esterification. Comparison of the result of methanol and ethanol, the results found ethanol gave higher FFA conversion than methanol in both type of starting materials. This result was consistent with the results in section 4.3.3 due to increasing FFA solubility in longer hydrocarbon chain of alcohol.

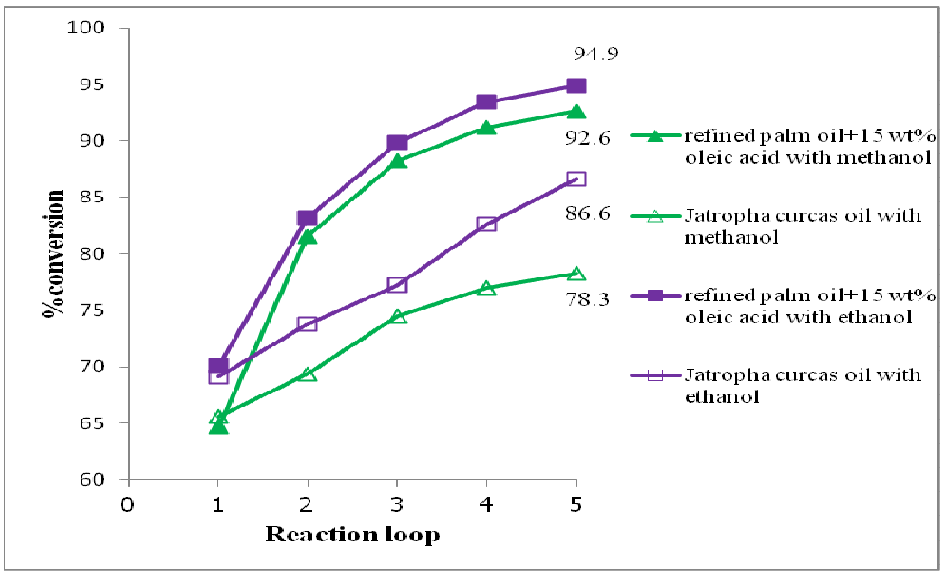

Figure 4.16 Comparison of FFA conversion between oleic acid in RPO and *Jatropha curcas* oil with methanol and ethanol.

The FFA conversion of leaching solution test in catalyst was shown in Table 4.17. The pellet catalyst was immersed in methanol 1 hour. After that, methanol was used as reactant in batch reactor which this esterification gave 34.7% FFA conversion (no catalyst). In comparison with blank reaction, the acid leaching solution test gave higher FFA conversion because partial acid leaching of catalyst to methanol could accelerate esterification.

Table 4.17 Test leaching of bentonite catalyst in esterification of FFA with methanol in batch reactor.

Reaction	%FFA	%conversion
Blank reaction (no catalyst)	12.3	16.0
Leaching solution test (no catalyst)	9.8	34.7
Catalyst 10 % (w/w)	1.7	88.7

Reaction condition: mole ratio of oil to methanol 1:23, catalyst 10% (w/w) and reaction time 1 hour.

4.3.9 Activity of recycled treated bentonite

The recycled catalyst was determined physical properties using XRD, ATR-IR and acid-base titration. The XRD patterns of reused material showed in Figure 4.17. In comparison, fresh and reused treated bentonite, the reused catalyst exhibited the absence of montmorillonite peak at d_{001} and d_{020} due to phase transformation. Moreover, the intensity of quartz or silica increased after reaction due to transformation of silica phase in montmorillonite. In addition, the acid value of reused treated bentonite decreased from 2.0 to 0.9 mmol/g due to acid leaching from clay structure. Meanwhile, IR spectrum of reused treated bentonite in Figure 4.18 displayed low intensity of H-O-H stretching and bending vibration band at 3132 and 1640 cm^{-1} which was consistent with the decreasing of acid value. From the results of characterization, the properties of reused catalyst were changed to reduce catalytic activity in esterification that shown in Table 4.18 and Figure 4.19.

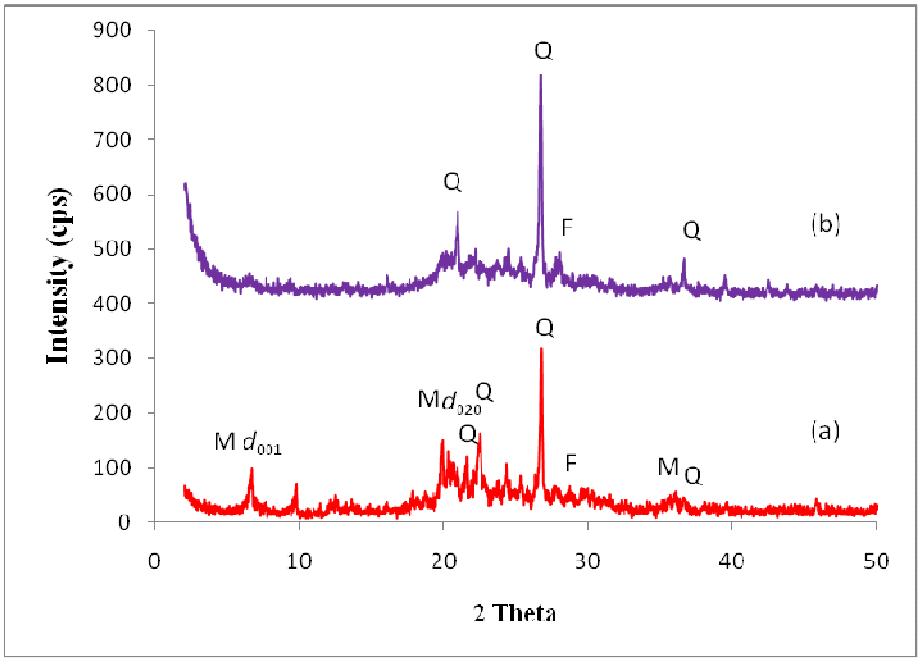

Figure 4.17 XRD patterns of (a) treated bentonite and (b) reused treated bentonite (M-montmorillonite, Q-quartz and F-feldspars).

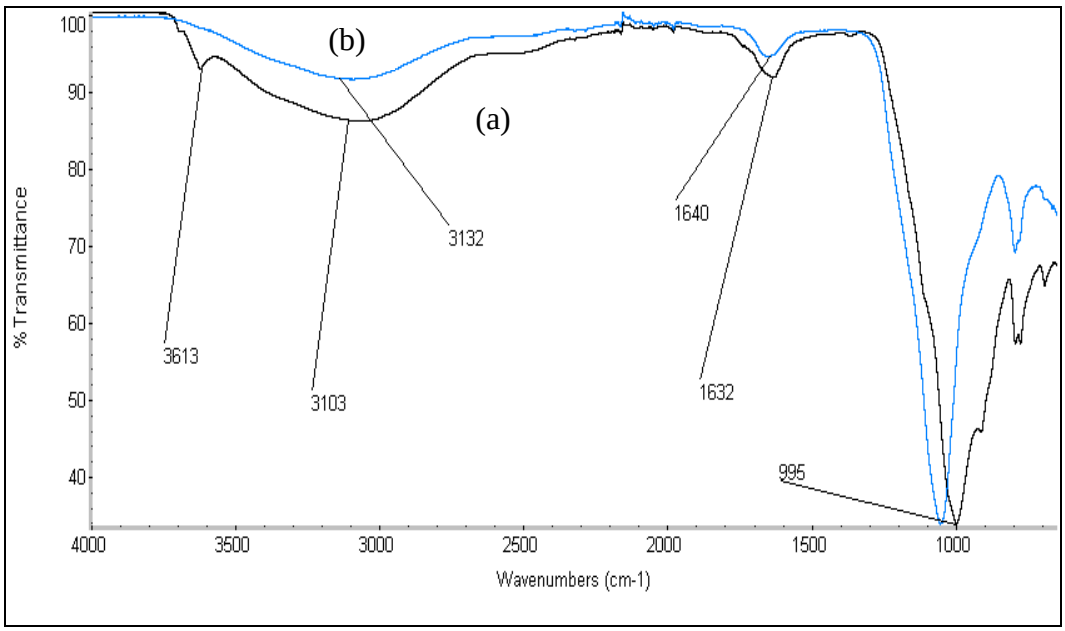

Figure 4.18 ATR-IR spectra of (a) treated bentonite and (b) reused treated bentonite.

The study of treated bentonite reusability was performed by feeding methanol into packed-bed reactor for catalytic washing until methanol appeared as a clear solution. This reaction was studied the catalytic activity of reused catalyst as shown in Table 4.18 and Figure 4.19. When comparison the activities with fresh catalyst, the FFA conversion was decreased in all loops due to decreasing of acid value, decreasing H-O-H stretching vibration band at 3103 cm^{-1} and phase transformation of montmorillonite in clay structure. The highest FFA conversion was 73.3% (%FFA as 4.0%) in the 5^{th} loop with mole ratio of oil to methanol as 1:54 with catalytic height 25 cm at reaction temperature 60^{o}C. Furthermore, pellets of reused catalyst were not broken after reaction.

Table 4.18 Comparison of FFA conversion between fresh and reused catalyst in esterification of oleic acid with methanol.

Sample	FFA, as oleic acid (%conversion)	
	Treated bentonite	
	Fresh	Reused
Refined palm oil+15 wt% oleic acid	13.6	15.0
1st loop	4.8(64.7)	6.4(57.3)
2nd loop	2.5(81.6)	6.0(60.0)
3rd loop	1.6(88.2)	5.1(66.0)
4th loop	1.2(91.2)	4.6(69.3)
5th loop	1.0(92.6)	4.0(73.3)

Reaction condition: mole ratio of oil to methanol as 1:54, catalytic height 25 cm, reaction temperature 60°C, LHSV 1.5 hr^{-1}.

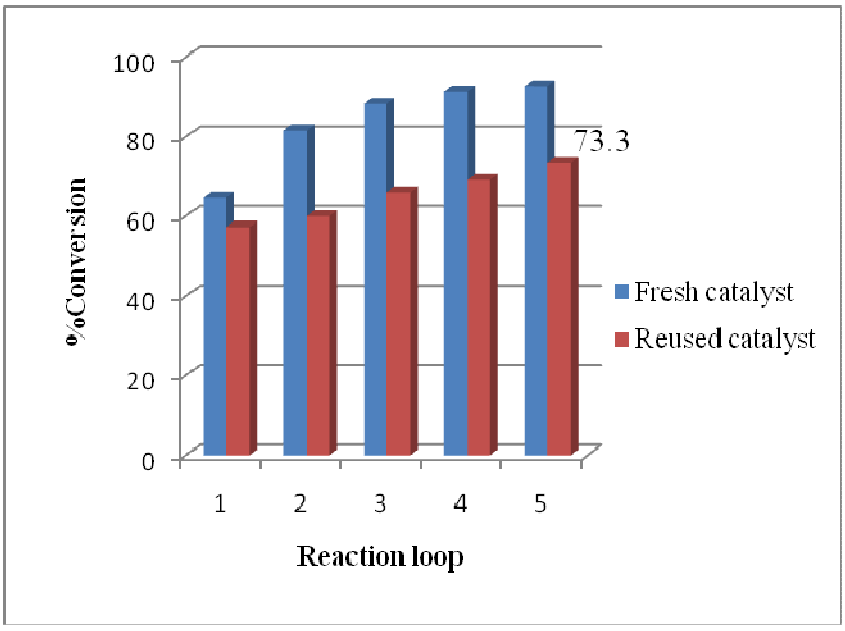

Figure 4.19 Comparison of FFA conversion between fresh and reused catalyst.

CHAPTER V
CONCLUSIONS

Sodium bentonite clay was successfully treated by ion-exchange method with 0.5 M H_2SO_4. The chemical composition of sodium bentonite mainly contained SiO_2 and Al_2O_3. The cation (Na^+, Ca^{2+}, Mg^{2+}, Al^{3+}, K^+, and Fe^{3+}) was decreased after acid treatment. The increase in the SO_3 was obtained from sulfuric solution in acidify process that agreement with increasing acid value. From XRD patterns, the acid treatment process could decrease montmorillonite phase at d_{001} and d_{020}. Moreover, ATR-IR spectrum of treated bentonite showed higher intensity of H-O-H stretching band at 3103 cm^{-1} which exhibited higher acid value. From SEM technique, the material after acid modification illustrated well-define and increased the depth of surface layer. The N_2 adsorption-desorption isotherms and pore size distribution exhibited type II isotherm, a characteristic pattern of non-porous materials. Both TG and DTG curves of treated bentonite showed two steps weight loss which exhibited losing of physisorbed water and chemisorbed inorganic substance.

Esterification of 15 wt% oleic acid in refined palm oil with alcohol using treated bentonite cylinder catalyst over a continuous packed bed reactor. The optimum condition was obtained using alcohol to oil mole ratio as 54, catalytic height 25 cm (13.5 g) at 60°C for one-column reactor experiment which exhibited FFA conversion as 92.6% and 94.9% for esterification with methanol and ethanol, respectively. Meanwhile, two-column reactors could reduce the FFA content to lower than 1 wt%. Moreover, esterification condition of oleic acid was applied to *Jatropha curcas* oil for methanol and ethanol. The FFA conversions were 78.3% and 86.6% for methanol and ethanol, respectively. Esterification of ethanol gave higher FFA conversion than methanol due to increasing FFA solubility in longer hydrocarbon chain of alcohol. The FFA conversion of reused treated bentonite was decreased due to decomposition of montmorillonite mineral in structure of clay.

The suggestion for future work

1. To improve structural strength of treated bentonite by pillar clay method.
2. To develop catalytic extrusion processes by using high efficient extruder.
3. To explore the use of treated bentonite clay to other reactions such as transesterification.

REFERENCES

[1] World marketed energy consumption [Online]. Available from: http://www.fypower.org/pdf/EIA_AEO_2006.pdf [2011, July 15].

[2] Kamarudin, S.K., Yusuf, N.N.A.N., Yaakub, Z. Overview on the current trends in biodiesel production. *Energy Convers. Manage*. 52(2011): 2741.

[3] Royon, D., Daz, M., Ellenrieder, G., and Locatelli. Enzymatic production of biodiesel from cotton seed oil using *t*-butanol as a solvent. *Bioresour. Technol.* 98(2006): 648.

[4] Yadav, G. D., and Lathi, P. S. Lipase catalyzed transesterification of methyl acetoacetate with *n*-butanol. *J. Mol. Cat. B.* 32(2005): 107.

[5] Aracil, J., Vicente, G., and Martinez, M. Integrated biodiesel production: a comparison of different homogeneous catalysts systems. *Bioresour. Technol.* 92(2004): 297.

[6] Chongkhong, S., Tongurai, C., and Chetpattananondh, P. Continuous esterification for biodiesel production from palm fatty acid distillate using economical process. *Renew Energ*. 34(2009): 1059.

[7] Zhang, L., Sun, P., Sun, J., Yao, J., and Xu, N. Continuous production of biodiesel from high acid value oils in microstructured reactor by acid-catalyzed reactions. *Chem Eng J.* 162(2010): 364.

[8] Park, Y. M., Lee, D. W., Kim, D. K., Lee, J. S., and Lee, K. Y. The heterogeneous catalyst system for the continuous conversion of free fatty acids in used vegetable oils for the production of biodiesel. *Catal Today*. 131(2008): 238.

[9] Murugesan, V., Chandrasekar, G., Hartmann, M., and Palanichamy, M. Extrusion of AlSBA-15 molecular sieves: An industrial point of view. *Catal Commun*. 8(2007): 457.

[10] Melero, J. A., Iglesias, J., Sainz-Pardo, J., Frutos, P., and azquez, S. Bl. Agglomeration of Ti-SBA-15 with clays for liquid phase olefin epoxidation in a continuous fixed bed reactor. *Chem Eng J.* 139(2008): 631.

[11] Peng, B. X., Shu, Q., Wang, J. F., Wang, G. R., Wang, D. Z., and Han, M. H. Biodiesel production from waste oil feedstocks by solid acid catalysis. *Process Saf Environ*. 86(2008): 441.

[12] Toshikuni, Y., Naomi, S-K., Takahiro, T., Kouhei, C., and Masaki, K. Simple continuous production process of biodiesel fuel from oil with high content of free fatty acid using ion-exchange resin catalysts. *Energ Fuel.* 24(2010): 3634.

[13] Pirola, C., Bianchi, C.L., Boffito, D.C., Carvoli, G., and Ragaini, V. Vegetable oil deacidification by Amberlyst:study of the catalyst lifetime and a suitable reactor configuration. *Ind. Eng. Chem. Res.* 49(2010): 4601.

[14] Kusakabe, K., Son, S.M., and Kimura, H. Esterification of oleic acid in a three-phase, fixed-bed reactor packed with a cation exchange resin catalyst. *Bioresour. Technol.* 102(2011): 2130.

[15] Vijayakumar, B., Mahadevaiah, N., Nagendrappa, G., and Jai Prakash, B.S. Esterification of stearic acid with *p*-cresol over modified Indian bentonite clay catalysts. *J. Porous Mater*.(2011)

[16] Trabelsi, M., Neji, S.B., and Frikha, M.H. Esterification of fatty acids with short-chain alcohols over commercial acid clays in a semi-continuous reactor. *Energies*. 2(2009): 1107.

[17] Srivastava, A., and Prasad, R. Triglyceride-based diesel fuels. *Renewable and Sustainable Energy Review.* 4(2000): 111.

[18] Tyson, K. S. Biodiesel handing and use guidelines. National Renewable Energy Laboratory, Department of Energy, CO.USA. (2001), NREL/TP-580-30004, Available from: http://www.agriculture.state.ia.us,INTERN.

[19] ประกาศกรมธุรกิจพลังงาน เรื่อง กำหนดลักษณะและคุณภาพของไบโอดีเซลประเภทเมทิลเอสเทอร์ของกรดไขมัน. ราชกิจจานุเบกษา (2548), 122 (ตอนพิเศษ 70 ง).

[20] Hanna, M. A., and Ma, F. Biodiesel production: review. *Bioresour. Technol.* 70 (1999): 1.

[21] Naik, S.N., Meher, L.C., and Vidya Sagar, D. Technical aspects of biodiesel production by transesterification: a review. *Renew. Sustain. E. Rev.* 10(2004): 1.

[22] Nesaretnam, K., Muhammad, B., Chong, C. L., and Tan, Y. A. Selected readings on palm oil and its uses, Kuala Lumpur, Palm Oil Research Institute of Malaysia, 1994.

[23] Unsaturated fatty acids [Online]. Available from: http://www.en.wikipedia.org/wiki/Fatty acid [2011, August 2].

[24] Sampattagul, S., Suttibut, C., Yucho, S., and Kiatsiriroat, T. Life Cycle Management of Jatropha Bio-Diesel Production in Thailand. Faculty of Engineering, Chiang Mai University.

[25] Ramesh, D., Samapahrajan, A., and Venkaachalam, P. Production of biodiesel from *jatropha curcas* oil by using pilot biodiesel plant. Agrl. Engg. College & Research Institute, Tamil Nadu Agricultural University, India.

[26] *Jatropha curcas Linn* [Online]. Available from: http://www.jatrogreentech.com/modules/wfchannel/index.php?pagenum=7 [2011, July 15].

[27] Activation energy [Online]. Available from: http://www.en.wikipedia.org/wiki/Activation energy [2010, February 14].

[28] Lepage, J. F., Cosyns, J., and Courty, P. Applied Heterogeneous catalysis: Design Manufacture and Use of solid catalysts, Technip, Paris, 1987.

[29] Noemi, M. N., and Konya, J. Interfacial chemistry of rocks and soils, Taylor and Francis Group, 2010.

[30] Adamis, Z., Fodor, J., and Williams, R. B. Bentonite, kaolin, and selected clay minerals, World Health Organization Geneva, 2005.

[31] Sposito, G., Park, S., and Sutton, R. Molecular simulations of clay mineral surface geochemistry. *Annual Report Basic Energy Sciences.* 1998.

[32] Types of bentonite [Online]. Available from: http://www.en.wikipedia.org/wiki/Bentonite [2011, July 25].

[33] Application of bentonite [Online]. Available from: http://www.healingdaily.com/detoxification-diet/bentonite-clay.htm [2011, July 20].

[34] Rossman, F. G., and Carel, J. V. O. Colloid and surface properties of clays and related minerals, Marcel Dekker, 2002.

[35] Moore, D. M., and Reynolds, Jr. R. C. X-Ray Diffraction and the Identifiation and Analysis of Clay Minerals, New York, Oxford University Press, 1989.

[36] Basic operating principles of the sorptomatic [Online]. Available from: http://www.saf.chem.ox.ac.uk./Instruments/BET/sorpoptprin [2011, August 2].

[37] Analysis software user's manual, BELSORP, BEL JAPAN, INC.

[38] Gabriel, B.L. SEM: A User's Manual for Material Science, Ohio: American Society for Metal, 1985.

[39] Theory XRF [Online]. Available from: http://www.learnxrf.com/BasicXRFTheory.htm [2011, Mar 1].

[40] Thermogravimetric Analysis (TGA) [Online]. Available from: http://www.kt.dtu.dk/~vigild/200504 melitek/tga.htm [2011, July 25].

[41] Thermogravimetric Analysis (TGA) [Online]. Available from: http://www.en.wikipedia.org/wiki/Thermogravimetric_analysis [2011, July 25].

[42] Nanda, S. Reactors and fundamentals of reactors design for chemical reaction. PHARMACEUTICAL ENGINEERING, 2008.

[43] Mbaraka, I. K., Radu, D. R., Lin, V. S. Y., and Shanks, B. H. Organosulfonic acid-functionalized mesoporous silicas for the esterification of fatty acid. *J. Catal.* 219(2003): 329.

[44] Muserref, O. Swelling and cation exchange capacity relationship for the samples obtained from a bentonite by acid activations and heat treatments. *Appl. Clay Sci.* 37(2007): 74.

[45] Majid, H-A., Jazayeri, S-H., Mohammad, G., and Ahmad, N. Experimental characterizations and swelling studies of natural and activated bentonites with their commercial applications. *J. Chem. Eng. Jpn.* 44(2011): 67.

[46] Liu, Z., Md, A. U., and Sun, Z. FT-IR and XRD analysis of natural Na-bentonite and Cu(II)-loaded Na-bentonite. *Spectrochim. Acta, Part A.* 79(2011): 1013.

[47] Hulya, N., Muserref, O., and Yuksel, S. The effect of sulphuric acid activation on the crystallinity, surface area, porosity, surface acidity, and bleaching power of a bentonite. *Food Chem.* 105(2007): 156.

[48] Muserref, O., Yuksel, S., and Tulay, A. The effect of acid activation on some physicochemical properties of a bentonite. *Turk J Chem*. 26(2002): 409.

[49] Xinfeng, X., Yanfen, D., Zhongzhong, Q., Feng, W., Bin, W., Hu, Z., Shimin, Z., and Mingshu, Y. Degradation of poly(ethylene terephthalate)/clay nanocomposites during melt extrusion: Effect of clay catalysis and chain extension. *Polym. Degrad. Stab.* 94(2009): 113.

[50] Venkatathri, N. Characterization and catalytic properties of a naturally occurring clay, bentonite. *Bull. Catal. Soc. India.* 5(2006): 61.

[51] Singh, C.P., Kumar, G., Kumar, D. Singh. S., Kothari, S., and Bhatt, S. Continuous low cost transesterification process for the production of coconut biodiesel. *Energies*. 3(2010): 43.

[52] Marchetti, J.M., Miguel, V.U., and Errazu, A.F. Heterogeneous esterification of oil with high amount of free fatty acids. *Fuel*. 86(2007): 906.

[53] Yaohui, F., Aiqing, Z., Jianxin, L., and Benqiao, H. A continuous process for biodiesel production in a fixed bed reactor packed with cation-exchange resin as heterogeneous catalyst. *Bioresour. Technol.* 102(2011): 3607.

APPENDICES

1. Calculation of free fatty acid conversion

Free fatty acids (FFA, as oleic acid) was analysed by potentiometric measurement (Mettler Toledo T50). The percentage conversion of free fatty acid was calculated as follows:

$$\text{Conv} = \frac{a_i - a_t}{a_i} \times 100 \qquad \text{(A-1)}$$

where;

Conv = conversion of free fatty acid (as oleic acid)

a_i = initial acid value

a_t = acid value at time

Acid value was calculated as follows:

$$a_x = \frac{V \times 28.2 \times c}{W} \qquad \text{(A-2)}$$

where;

a_x = acid value at other time

V = volume of titrant (ml)

c = concentration of titrant (mole/l)

W= weight of sample (g)

2. Calculation of Liquid Hourly Space Velocity

Liquid Hourly Space Velocity, which is defined in the equation below:

$$LHSV = \frac{T \times 60\ (min)}{V \times 1\ (hr)} \qquad (A\text{-}3)$$

where;

LHSV = Liquid Hourly Space Velocity (hr^{-1})

T = total feed rate of reactant (ml/min)

V= volume of reactor (cm^3)

Volume of reactor was calculated as follows:

$$V = ¶ \times r^2 \times h \qquad (A\text{-}4)$$

where;

V = volume of reactor (cm^3)

r = radius of reactor (cm)

h = height of reactor (cm)

Start dried bentonite ($1.2\ cm^3/1.0\ g$)	After add MeOH ($1.2\ cm^3/1.0\ g$)	After 1 week ($1.2\ cm^3/1.0\ g$)

Figure A-1 Swelling test of treated bentonite.

Start dried bentonite+cellulose (95:5) ($1.3\ cm^3/1.0\ g$)	After add MeOH ($1.3\ cm^3/1.0\ g$)	After 1 week ($1.3\ cm^3/1.0\ g$)

Figure A-2 Swelling test of mixed treated bentonite with cellulose in ratio 95:5.

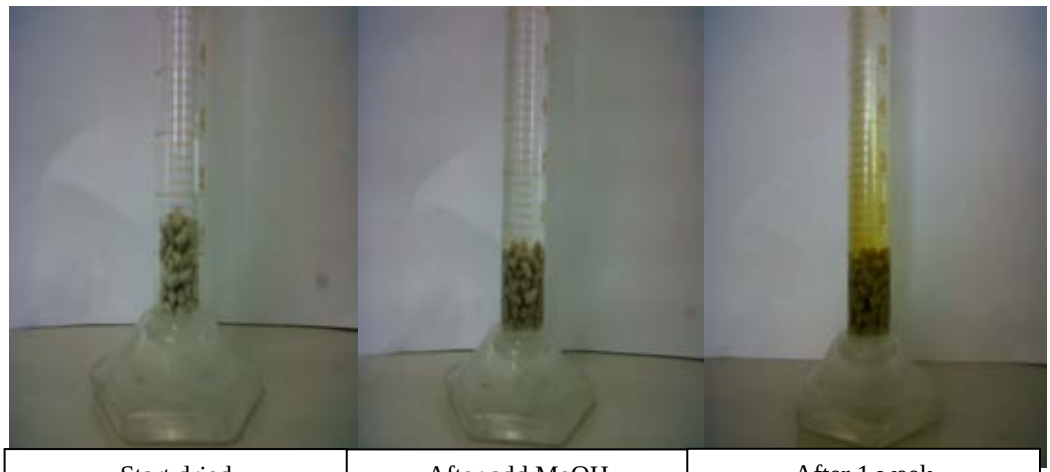

Start dried bentonite+cellulose (90:10) (1.3 cm^3/1.0 g)	After add MeOH (1.3 cm^3/1.0 g)	After 1 week (1.3 cm^3/1.0 g)

Figure A-3 Swelling test of mixed treated bentonite with cellulose in ratio 90:10.

Start dried bentonite+cellulose (85:15) (1.4 cm^3/1.0 g)	After add MeOH (1.4 cm^3/1.0 g)	After 1 week (1.4 cm^3/1.0 g)

Figure A-4 Swelling test of mixed treated bentonite with cellulose in ratio 85:15.

Start dried bentonite+SBA-15-Pr-SO_3H (90:10) (1.3 cm^3/1.0 g)	After add MeOH (1.3 cm^3/1.0 g)	After 1 week (1.3 cm^3/1.0 g)

Figure A-5 Swelling test of mixed treated bentonite with SBA-15-Pr-SO_3H in ratio 90:10.

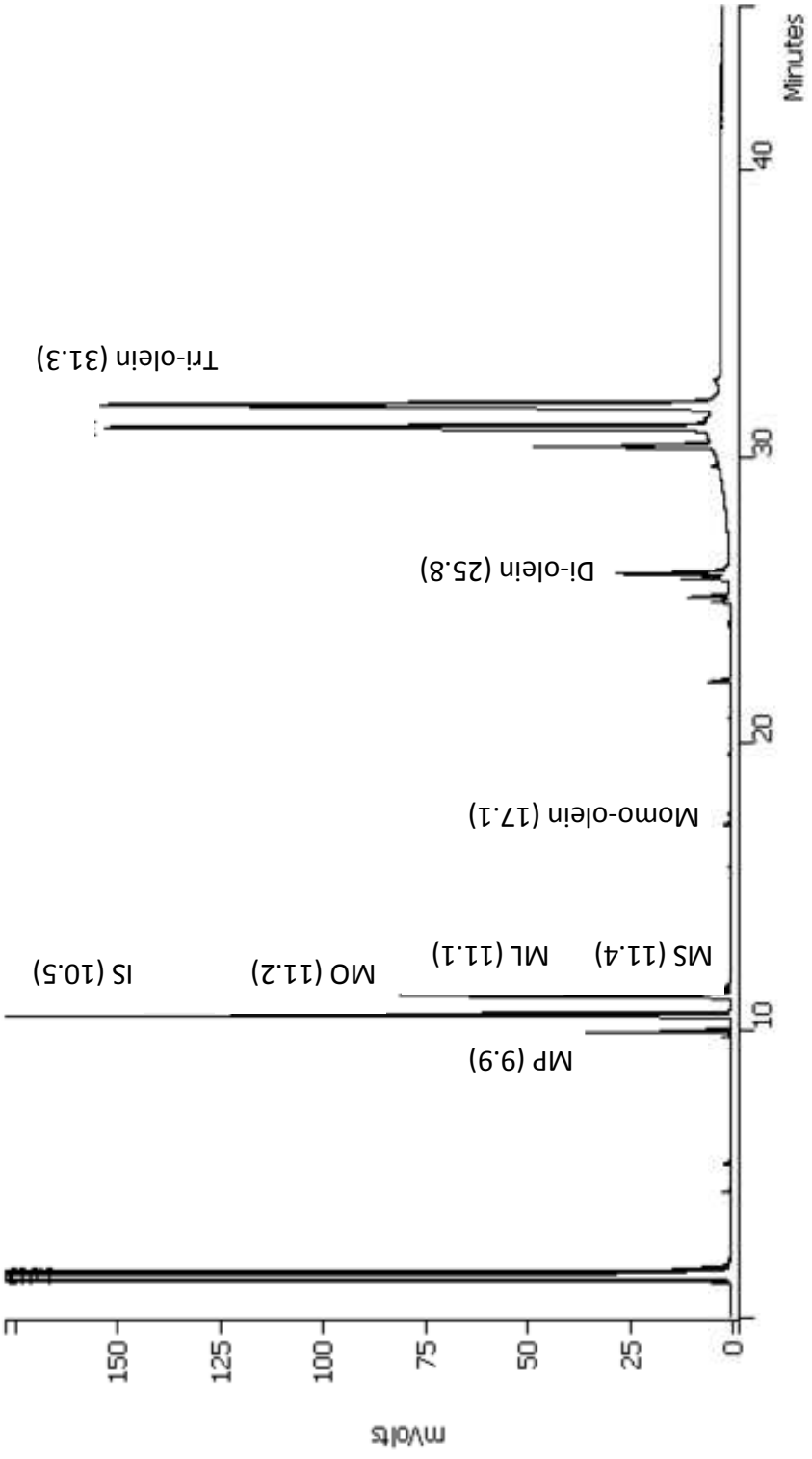

Figure A-6 Gas chromatogram of methyl ester from esterificaton of refined palm oil at 60^{o}C

VITAE

Mr. Somyod Kedpokasiri was born on August 2, 1986 in Bangkok, Thailand. He received a Bachelor Degree of Science, major in Chemistry from Thammasat University in 2008. Since 2009 he has been a graduate student in the program of Petrochemistry and Polymer Science, Faculty of Science, Chulalongkorn University and completed his Master of Science Degree in 2011.

In 30 June-1 July 2011, he participated in International Symposium on Material Science Engineering and Energy Technology, Faculty of Science and Technology, Thammasat University, Pathumtani, Thailand approval of proceeding and oral presentation in the title of “Esterification of biodiesel production using Amberlyst-15 catalyst in continuous packed bed reactor”.

His present address is 139 Soi Somdejprapinklao2, Bangyikhan, Bangphlat, Bangkok, Thailand 10700.